

ARTICLE OPEN



Structural covariance network topology in individuals at clinical high risk for psychosis: the ENIGMA-CHR Study

Siwei Liu^{1,2}, Ingrid Agartz^{3,4,5,6}, Paul Allen^{7,8}, G. Paul Amminger^{9,10}, Ole A. Andreassen^{5,11}, Peter Bachman¹², Inmaculada Baeza^{13,14,15,16}, Helen Baldwin^{17,18,19}, Cali F. Bartholomeusz^{9,10}, Stefan Borgwardt^{20,21}, Sabrina Catalano²², Xiaogang Chen^{23,24}, Kang Ik K. Cho²⁵, Sunah Choi²⁶, Tiziano Colibazzi^{27,28}, Rebecca E. Cooper^{12,29}, Cheryl M. Corcoran^{30,31}, Vanessa L. Cropley^{9,10}, Lieuwe de Haan^{32,33}, Camilo de la Fuente-Sandoval³⁴, Montserrat Dolz^{13,35,36}, Bjørn H. Ebdrup^{37,38}, Adriana Fortea^{13,16,39}, Paolo Fusar-Poli^{40,41,42,43}, Louise Birkedal Glenthøj⁴⁴, Birte Yding Glenthøj^{37,38}, Shalaila S. Haas³⁰, Holly K. Hamilton^{45,46,47}, Kristen M. Haut⁴⁸, Rebecca A. Hayes¹², Ying He²³, Karsten Heekeren^{49,50}, Wenche ten Velden Hegelstad^{51,52}, Christine I. Hooker⁴⁸, Leslie E. Horton²², Daniela Hubl⁵³, Wu Jeong Hwang⁵⁴, Michael Kaess^{55,56}, Kiyoto Kasai^{57,58,59}, Naoyuki Katagiri⁶⁰, Minah Kim^{61,62}, Jochen Kindler⁵⁶, Mallory J. Klaunig⁶³, Shinsuke Koike^{58,64}, Tina D. Kristensen³⁷, Yoo Bin Kwak²⁶, Jun Soo Kwon^{26,61,62}, Stephen M. Lawrie⁶⁵, Irina Lebedeva⁶⁶, Imke LJ Lemmers-Jansen^{17,67}, Pablo León-Ortiz³⁴, Ashleigh Lin⁶⁸, Rachel L. Loewy⁴⁶, Xiaoqian Ma²³, Daniel H. Mathalon^{46,69}, Patrick McGorry^{9,10}, Philip McGuire⁷⁰, Chantal Michel⁵⁶, Romina Mizrahi^{71,72}, Masafumi Mizuno⁷³, Paul Møller⁷⁴, Ricardo Mora-Durán⁷⁵, Daniel Muñoz-Samons^{35,36}, Barnaby Nelson^{9,10}, Takahiro Nemoto⁷⁶, Merete Nordentoft⁷⁷, Dorte Nordholm⁷⁷, Maria A. Omelchenko⁷⁸, Lijun Ouyang^{23,24,79}, Christos Pantelis^{80,81,82}, Jose C. Pariente⁸³, Jayachandra M. Raghava^{37,84}, Paul E. Rasser^{85,86}, Franz Resch⁸⁷, Francisco Reyes-Madrigal³⁴, Luis F. Rivera-Chávez³⁴, Jan I. Rössberg⁶, Wulf Rössler^{50,88}, Dean F. Salisbury²², Daiki Sasabayashi^{89,90}, Ulrich Schall^{85,91}, Jason Schiffman⁹², Andre Schmidt²⁰, Lukasz Smigielski^{50,93}, Mikkel E. Sørensen³⁷, Gisela Sugranyes^{13,14,15,16}, Michio Suzuki^{89,90}, Tsutomu Takahashi^{89,90}, Christian K. Tamnes^{94,95}, Jinsong Tang^{96,97}, Anastasia Theodoridou⁵⁰, Sophia I. Thomopoulos⁹⁸, Alexander S. Tomyshev⁶⁶, Jordina Tor^{35,36}, Peter J. Uhlhaas^{99,100}, Tor G. Værnes^{6,101}, Therese AMJ van Amelsvoort¹⁰², Dennis Velakoulis^{103,104}, Esther Via^{35,36}, Sophia Vinogradov⁴⁵, James A. Waltz¹⁰⁵, Christina Wenneberg⁷⁷, Lars T. Westlye^{5,6,106}, Stephen J. Wood^{9,10,107}, Hidenori Yamasue¹⁰⁸, Liu Yuan^{23,24,79}, Alison R. Yung^{109,110}, Michael WL Chee^{1,2}, Paul M. Thompson⁹⁸, Dennis Hernaus¹⁰², Maria Jalbrzikowski^{12,29}, Jimmy Lee^{111,112}, Juan H. Zhou^{1,2,113} and ENIGMA Clinical High Risk for Psychosis Working Group*

© The Author(s) 2025

Brain network architecture is anticipated to influence future grey matter loss in individuals at Clinical High Risk (CHR) for psychosis. However, existing studies on grey matter structural network properties in CHR are scarce and constrained by small sample sizes. Here, we examined network topology differences comparing a) CHR versus healthy controls (HC); b) CHR who transitioned to psychosis (CHR-T) versus those who did not (CHR-NT); and c) different subsyndromes. We included structural scans from 1842 CHR individuals and 1417 HC individuals from 31 sites within the Enhancing Neuroimaging Genetics through Meta-Analysis (ENIGMA) consortium. At the global level, CHR individuals exhibited lower structural covariance ($q < 0.001$; Cohen's $d = 0.164$) and less optimal structural network configuration than HC (lower global efficiency and clustering coefficient, $d = 0.100, 0.087$, $q_s \leq 0.027$). Though no global difference between CHR-T and CHR-NT, network distinctiveness of the frontal and temporal surface area networks was higher in CHR-T than CHR-NT ($d = 0.223, 0.237$) and HC ($d = 0.208, 0.219$) ($q_s < 0.001$). Network distinctiveness of the frontal cortical thickness network was lower in CHR-T ($d = 0.218$, $q < 0.001$) than CHR-NT and HC ($d = 0.165$, $q < 0.001$). Importantly, higher network distinctiveness was associated with worse positive symptoms in CHR-NT (frontal surface area, $q = 0.008$, $R^2 = 0.013$) and at trend with worse negative symptoms in CHR-T (frontal thickness, $q = 0.063$, $R^2 = 0.049$). Further, the brief intermittent psychotic syndrome subgroup showed more severe network alterations. Together, brain structural networks inform symptoms and the risk of transition to psychosis in CHR individuals.

Molecular Psychiatry (2026) 31:1707–1722; <https://doi.org/10.1038/s41380-025-03304-6>

INTRODUCTION

Clinical High Risk for psychosis (CHR) describes a state characterized by young people who have a heightened risk of developing a psychotic disorder [1], with a 20–30% transition likelihood within

2–3 years [2, 3]. Subsyndromes include the attenuated positive symptom (APS) syndrome, the genetic risk for psychosis accompanied by a recent decline in functioning (GRD), and the brief intermittent psychotic syndrome (BIPS) [4, 5]. Decline in social

A full list of author affiliations appears at the end of the paper.

Received: 4 August 2024 Revised: 10 September 2025 Accepted: 7 October 2025

Published online: 22 October 2025

functioning, co-morbidity, and lower perceived quality of life are common, creating burden in the CHR state [6–9]. Preventive interventions could potentially ameliorate the high burden in CHR state and reduce the transition to psychosis [10, 11]. Discovering biomarkers based on brain abnormalities in CHR state will help identify those in need for indicated prevention [12].

Neuroimaging studies reveal widespread subtle structural abnormalities in CHR individuals, resembling those in psychotic disorders [13–21]. Using the largest pooled neuroimaging sample of CHR individuals to date, the Enhancing Neuroimaging Genetics through Meta-Analysis [ENIGMA] CHR working group found widespread cortical thinning in CHR individuals [13]. Those who later transitioned to psychosis (CHR-T) showed lower cortical thickness in fusiform, superior temporal, and paracentral regions than non-transitioners (CHR-NT) [13]. Smaller surface area in the right superior frontal, right superior temporal, and bilateral insular cortices distinguished CHR-T from healthy controls (HC) [18]. Additionally, both CHR individuals and schizophrenia patients show greater intra-group variability in morphometric profiles than HC [14, 22], suggesting disease-related divergence. If regions diverge differently, greater variability in CHR may weaken inter-regional covariance. If regions diverge similarly, this variability may reflect shared patterns of abnormal network organization or reorganization.

Evidence from patients with schizophrenia and at-risk individuals suggests that psychotic disorders may compromise optimal brain network configurations [23–25]. Brain networks can be identified using structural covariation in grey matter, an established method characterising concomitant morphometric variations (e.g., thickness and gyrification) among distributed regions [26]. Covariation between regions follows the homophilic principle, where morphometrically similar regions are likely axonally connected [26, 27]. Regions within structural covariance networks share maturation trajectories [28, 29], as well as functional [30–32] and transcriptomic [33] similarity, and their disruption may indicate developmental alterations and/or pathological development [23, 34]. Importantly, the topology of neurotypical brain networks exhibits small-world architecture, balancing local segregation and global integration through hierarchical modular structures [35, 36]. This architecture supports cognition [37], remains robustness against focal atrophy, and limits the spread of abnormalities [38, 39] (supplementary background). However, globally, schizophrenia shows lower integration [24, 40, 41] and higher segregation [40, 42] compared to controls, while bipolar disorder has intermediate integration loss [24]. In schizophrenia, frontal networks are weakened and less hierarchical than controls, increasing integration [36, 40, 43], whereas posterior networks fragment into smaller subnetworks, enhancing segregation [36, 40, 41, 43–45].

Few studies have used graph theory to examine structural brain alterations in individuals at risk for psychosis. Drakesmith and colleagues [46] observed lower global efficiency (lower integration) among healthy individuals with psychotic-like experiences than those without. Sandini and colleagues [47] reported higher modularity and clustering coefficient (increased segregation) in individuals with 22q11.2 Deletion Syndrome and attenuated psychotic symptoms, compared to those without symptoms and healthy controls. In CHR individuals, Das and colleagues [48] observed lower small-worldness, lower integration, and higher segregation in CHR-T than CHR-NT. In contrast, individuals at familial risk for psychosis without psychotic symptoms showed no global network disruptions [49–51], despite frontal nodal differences and topological alterations during infancy [52]. This suggests that the structural network topographical alterations may be state-dependent, but previous studies with small or moderate sample sizes leaves it unclear whether structural network topology reliably differentiates individuals at risk for psychosis or predicts transition to psychosis.

Understanding structural network topology in CHR is crucial, as the network hypothesis of schizophrenia suggests that structural deficits propagate through strongly connected regions [53–56]. Initial focal atrophy may spread within the same network due to disruptions of signalling, trophic support, and/or neurotransmitter systems [57], suggesting network architecture as a potential roadmap for pathological progression. Regions covarying with existing atrophy may be the next affected. Evidence supporting the network hypothesis spans first-episode, chronic, and treatment-resistant schizophrenia [55, 56, 58]. For example, Regional deficits can be predicted by deficits of neighboring regions and their connectivity [56, 58]. These network-driven structural patterns align with cytoarchitectonic classes [58] such as the limbic class [59, 60], linking pathology across different system levels.

Furthermore, the brain's small-world and modular architecture implies that pathological spread occurs in stages [61] (supplementary background). Optimal small-world configuration reduces network vulnerability to focal atrophy in networks (stage 1) [62, 63]. Network distinctiveness (characterized by within-network specialization and between-network segregation) constrains atrophy within networks (stage 2) [64] and delays cascading effects that would result in multinet network failures (stage 3), as seen in schizophrenia [65]. Therefore, we expected network distinctiveness to vary across breakdown stages: lower in stage 1, higher in stage 2, and lower again in stage 3, driven by within-network covariance in the stage 1 and 2 and by between-network covariance in stage 3. To fully understand pathological spread, it is essential to consider network distinctiveness alongside both within- and between-network covariance.

We aimed to elucidate structural covariance network alterations in CHR individuals at global level and local network levels using a large ENIGMA CHR working group. At the global level, we measured covariation strength, integration, segregation, and the balance between segregation and integration, expecting disruptions in CHR individuals compared to HC due to subthreshold symptoms and functional decline [1, 4, 5, 66]. At the network-level, we examined network distinctiveness using the system segregation index [39], which quantifies the within- and between-network covariance difference normalised by the within-network covariance. Based on prior studies [40, 41, 43], we hypothesized that network distinctiveness would be associated with future transition status, depending on network breakdown stages [54, 61]. Lastly, we tested the relationship between network distinctiveness and symptom severity in CHR [47], and explored heterogeneity across CHR subsyndromes.

METHODS

Participants

Our final imaging sample (Table 1) comprised 1282 healthy controls (700 males) and 1582 CHR individuals (811 males) from ENIGMA-CHR working group [13]. The mean ages [ranges] were 22.2 [12.0, 39.9] and 20.6 [9.5, 39.8], respectively. The CHR group comprised 229 CHR-T (14.5%), 1102 CHR-NT and 251 unknown transition status. Median follow-up durations [ranges] were 158 [2–316], 152 [2–325], and 57 [1–327] months, respectively (eMethod 1). Among CHR individuals with subsyndrome classification, 1325 met criteria for APS (Attenuated Positive Symptom Syndrome via Structured Interview for Prodromal Symptoms, SIPS [4] or Attenuated Psychosis Group via Comprehensive Assessment of At Risk Mental States, CAARMS [5]), 235 for GRD (Genetic Risk and Deterioration Syndrome via SIPS or Vulnerability Group via CAARMS), and 79 for BIPS (Brief Intermittent Psychotic Symptom Syndrome via SIPS or Brief Limited Intermittent Psychotic Symptoms Group via CAARMS) (eTable 2–5). All 31 sites obtained local institutional review board approval. Informed written consent was obtained for all participants and/or their legal guardians.

Table 1. Demographics and clinical characteristics.

	HC (N = 1282)	CHR (N = 1582)	CHR-NT (N = 1102)	CHR-T (N = 229)
Demographics				
Sex (Male/Female)	700 / 582	811 / 771	558 / 544	127 / 102
Handedness (L/M/R)	80/23/971 ^{c,n}	171/28/1096 ^h	124/24/793 ^h	19/4/146
Age (years)	22.22 ^{c,t,n}	20.60 ^h	20.66 ^h	20.23 ^h
Follow-up duration in months, mean (SD)	113.67 (58.86) ^{c,t}	137.29 (76.40) ^h	135.56 (72.87) ^t	152.53 (75.73) ^{h,n}
Typical antipsychotics, N (%)	NA	27 (1.71)	23 (2.09)	2 (0.87)
Atypical antipsychotics, N (%)	NA	251 (15.87)	163 (14.79) ^t	37 (16.16) ⁿ
Subgroups^a, N (%)				
APS	NA	1325 (83.75)	933 (84.66) ^t	184 (80.35) ⁿ
BIPS	NA	79 (4.99)	45 (4.08) ^t	27 (11.79) ⁿ
GRD	NA	235 (14.85)	167 (15.15)	44 (19.21)
APS/GRD	NA	140 (8.85)	98 (8.89)	27 (11.79)
APS/BIPS	NA	36 (2.28)	21 (1.91) ^t	13 (5.68) ⁿ
BIPS/GRD	NA	9 (0.57)	5 (0.45)	4 (1.75)
APS/BIPS/GRD	NA	7 (0.44)	4 (0.36)	3 (1.31)
Unknown	NA	111 (7.02)	68 (6.17)	14 (6.11)
Clinical Measures^b				
Total SOPS positive symptom score, mean (SD)	NA	10.91 (4.72)	10.79 (4.76) ^t	12.15 (5.15) ⁿ
Total SOPS negative symptom score, mean (SD)	NA	12.67 (6.50)	12.71 (6.53) ^t	14.03 (7.00) ⁿ
Total SOPS disorganized symptom score, mean (SD)	NA	5.54 (3.53)	5.74 (3.55) ^t	6.40 (4.11) ⁿ
Total SOPS general symptom score, mean (SD)	NA	8.20 (4.42)	8.29 (4.42)	8.60 (4.61)
Total CAARMS positive symptom score, mean (SD)	NA	10.35 (4.12)	10.04 (4.17)	10.90 (4.25)
Total CAARMS negative symptom score, mean (SD)	NA	6.67 (3.72)	6.63 (3.64)	7.75 (4.33)
Total CAARMS cognitive change score, mean (SD)	NA	3.27 (1.91)	3.46 (1.77)	4.43 (1.99)
Total CAARMS emotional disturbance score, mean (SD)	NA	3.86 (2.48)	4.07 (2.55)	4.43 (1.72)
Total CAARMS behavioral change score, mean (SD)	NA	8.64 (4.49)	8.79 (4.35)	9.13 (6.56)
Total CAARMS motor/physical change score, mean (SD)	NA	2.92 (2.43)	3.00 (2.50)	4.00 (2.61)
Total CAARMS general psychopathology score, mean (SD)	NA	13.16 (6.44)	13.30 (6.35)	14.00 (9.76)

h, significantly different from the HC group; c, significantly different from the CHR group; t, significantly different from the CHR-T group; n, significantly different from the CHR-NT group. a, some participants met criteria for more than one subgroup; b, some participants had neither CAARMS nor SOPS scores. HC healthy controls, CHR clinical high risk, CHR-NT clinical high risk with no transition during follow-up, CHR-T clinical high risk who transitioned to psychosis during follow-up, L left, M mixed, R right, SD standard deviation, APS attenuated psychotic symptoms, BIPS brief (limited) intermittent psychotic symptoms, GRD genetic and risk deterioration syndrome, SOPS Scale of Psychosis-risk Symptoms, CAARMS Comprehensive Assessment of At Risk Mental States, NA not applicable.

Data acquisition and preprocessing

Data were preprocessed using the ENIGMA pipeline [13, 14]. T1 brain images (eMethod 2) were parcellated into 34 cortical regions per hemisphere based on Desikan-Killiany atlas [67] and 8 subcortical regions (eMethod 1 and eTable 10) using Freesurfer v6.0. Cortical thickness, surface area and subcortical volumes were extracted. The ENIGMA quality control protocol (<https://github.com/ENIGMA-git/ENIGMA-FreeSurfer-protocol>) was applied. Site and scanner-associated effects were corrected using NeuroCombat harmonisation [68], a batch-adjustment method based on the empirical Bayes framework and used by previous studies [13–17].

Structural covariance network construction

Following prior work [69], we constructed the structural covariance matrix using cortical thickness (CT), cortical surface area (SA) and subcortical volume (Fig. 1). CT and SA of the same brain region were treated as separate nodes due to their distinct genetics [70, 71], neurobiology [72–75], and maturation trajectories [76, 77] (see supplementary methods). Disruptions in SA and CT may reflect different pathological changes. Combining them into a covariance matrix reveals how morphometric features are organized by connectivity during neurodevelopment. Given that CT and SA mature differently across regions [78–80]—e.g., sensory and motor areas develop earlier than the association cortex [79, 81]—this approach captures developmental coordination, and disruptions thereof.

Due to practical considerations (supplementary methods), regional values including CT, SA, or subcortical volume were averaged across the two hemispheres [69], unless one was missing, in which case the available value from the other hemisphere was used. Each participant had 76 node values: 34 for CT, 34 for SA, and 8 for subcortical volume. Further, age, sex and brain size (mean CT for CT, total SA for SA, and total intracranial volume for subcortical volume) were regressed out. We controlled for brain size due to heterogeneous scaling of brain properties with brain size. Among others, SA, compared to CT, and associative cortices, compared to sensorimotor cortices, increase more rapidly with greater brain sizes [26, 82]. In light of these findings and the observation that CT and SA are affected differently in CHR individuals [13], we used morphometric-type specific brain size metrics (for SA and CT separately) to correct CT and SA measures in our covariance matrix to minimize bias (supplementary methods).

Next, means and standard deviations were calculated across controls. Each participant's node values were z-transformed by subtracting the control mean and dividing by the control standard deviation, with z-scores indicating relative thickness, surface area, or volume differences. Finally, node covariation, based on z-score differences, was calculated using the equation in Fig. 1 (eMethod 3), where high covariation reflects similar deviations from controls. Each participant's covariance matrix captured individualized patterns of brain morphology.

Construction of structural covariance network

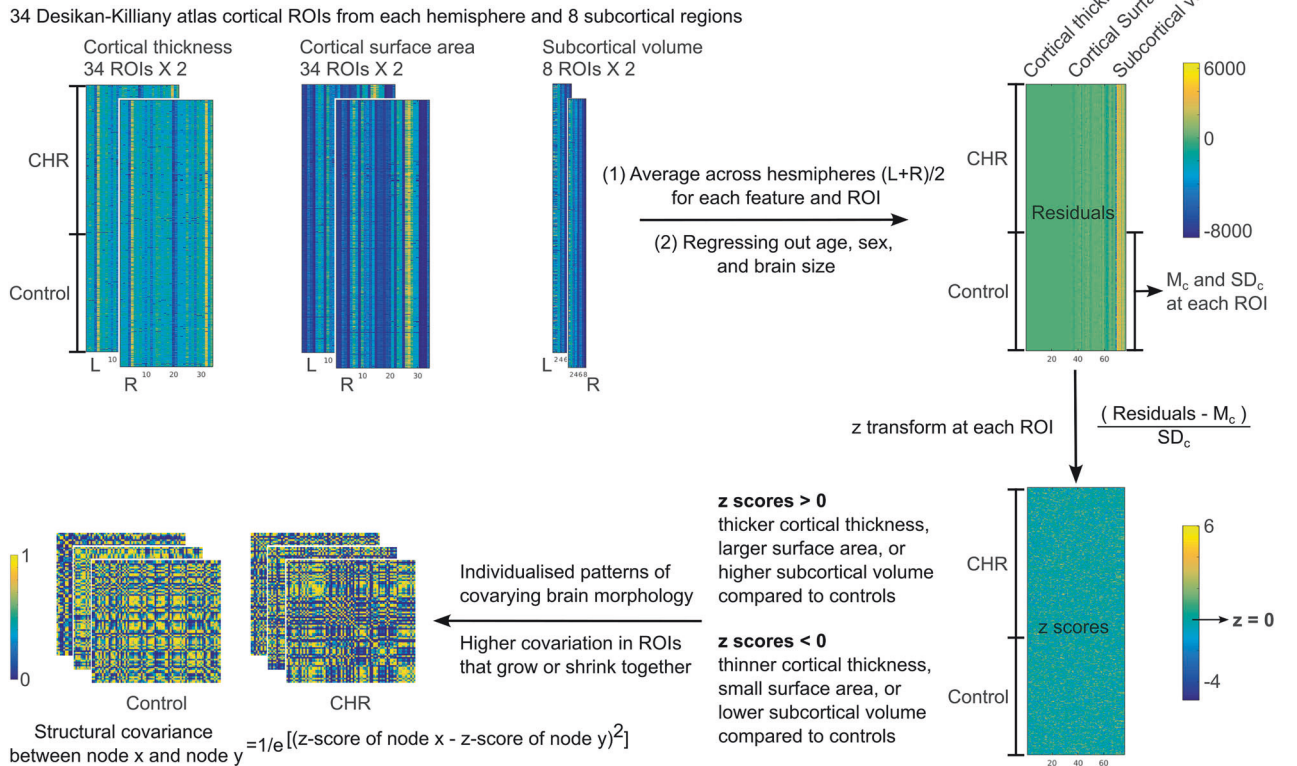


Fig. 1 Construction of structural covariance network. In line with previous work [44], we constructed the structural covariance matrix using cortical thickness, cortical surface area and subcortical volume. For each participant, the cortical thickness and cortical surface area estimates from 34 ROIs [42], and the volumes of 8 subcortical regions, from each hemisphere represented 76 nodes in the covariance matrix after averaging across hemispheres, covariate regression, z-score transformation and covariation calculation based on z-score differences. A high value in the covariance matrix suggests that two nodes differed similarly from the controls (i.e. growing or shrinking together). One covariance matrix was obtained for each participant, representing the individualised pattern of covarying brain morphology. ROI region of interest; CHR clinical high risk; L left; R right; M_c mean of the control group; SD_c standard deviation of the control group.

Global network topographical properties

Global topographical and network-level metrics were calculated in Matlab software (R2016b version, Brain Connectivity Toolbox). The structural covariance matrix from each participant was thresholded at sparsity levels from 0.10 to 0.25 (top 10–25%) in 0.01 steps [22, 44]. We calculated the following measures (also see supplementary methods): 1) global efficiency (information integration via shortest paths); 2) clustering coefficient (clustering among node neighbours), and 3) small-worldness (balance between clustering and path length). To avoid threshold bias, each graph measure was summarised by calculating the area under the curve (AUC) across sparsity levels (integral of metrics across sparsity levels via trapezoidal method) [83].

Community detection and network distinctiveness

The Desikan-Killiany atlas [67] is a gyral-based and does not directly map to intrinsic brain networks like the Yeo et al. parcellation [84]. To identify network architecture, we applied two-step community detection to structural covariance matrices (eMethod 5) [85]. Using the Louvain method [86], we performed community detection at individual (step 1) and group (step 2) levels across sparsity levels from 0.1 to 0.25 (step of 0.01). To determine community structure, we empirically assessed resolution (gamma). Individual-level detection used gamma 1 and 2, while group-level detection tested gamma 1 to 5, yielding 10 community structures. Median community size was plotted against gamma (eFigure 3) to identify elbow points, indicating stable resolution. We then compared node assignments to communities (from community detection) and the Desikan-Killiany parcel [67] assignment to intrinsic networks [84] using a

winner-takes-all approach. For example, the paracentral parcel was assigned to the somatomotor network since 82.1% of its vertices belonged to this network. Similarity between community and network assignments was evaluated using the Rand coefficient z-score [87], with higher values indicating greater alignment. Based on stability (elbow value) and similarity (Rand z), the optimal gamma was determined to be 2 at the group level and 1 at the individual level (eMethod 5, eFigure 3).

Finally, the network distinctiveness of each community within the community structure was measured by the system segregation index [39] (subtracting the mean between-community from the mean within-community covariance and dividing the difference by the mean within-community covariance).

Statistical analysis

Group comparisons. Statistical analyses were performed in R software (version 4.2.1). Group comparisons between CHR and controls used t-tests for continuous variables and Chi-square tests for categorical variables (except follow-up duration and symptom scores).

For subgroup comparisons, CHR individuals with unknown subgroup status (e.g. unknown psychosis transition status at follow-up, unknown APS status for APS subgroup comparison, etc.) were excluded. Due to highly imbalanced subgroup sizes, categorical variables were analyzed using the Rao-Scott corrected weighted Chi-square test [88] (survey, R package 4.2-1) and continuous variables with sample-sized-weighted analysis of variance (ANOVA) (except for follow-up duration and symptom scores). Initial comparisons included three-group analyses (e.g., controls vs. CHR-NT vs. CHR-T; controls vs. APS vs. non-APS), followed by pairwise comparisons for

significant results.

Symptom scores were analyzed using linear mixed modeling (LMM) with age and sex as fixed effects and site as a random effect (lmerTest, R package 3.1-3). LMM was also used for follow-up duration with site as a random effect.

Given the skewed distribution of global efficiency and system segregation indices (see Q-Q plots in eFigure 5), group comparisons for these measures used values within 3 median absolute deviations from the median across all communities and participants (eMethod 6).

Additionally, five sensitivity analyses were conducted: (1) To explore the medication influence, we repeated the comparisons additionally controlling for antipsychotic medication exposure (information available among 72.5% CHR-T and 87.1% CHR-NT individuals) for all the significant group differences. (2) To evaluate the influence of sites, we conducted leave-one-site-out (LOO) analyses (eMethod 7). (3) To examine whether the network findings were complementary to regional differences, we repeated the network-level group comparisons adding the mean within-community regional features (SA, CT or subcortical volume) as a covariate. (4) For communities with significant group differences in system segregation indices, within- and between-community covariance differences were also tested. (5) To evaluate the lateralisation effects, we repeated the group comparisons 1) without averaging the morphometric measures across the hemispheres using the current sample ($N = 2864$) and 2) using the smaller sample where all 152 morphometric values must be available ($N = 1735$).

Association between brain metrics and symptom scores. To examine the clinical implications of group differences, we used LMM to test the association between symptom scores and the brain metrics showing significant group differences, including fixed effects of brain metric, age and sex and the random effect of site. For transition-related brain metrics, we included both the main effect and the interaction with transition group to rule out confounding by group differences. Because most sites used either Scale of Psychosis-risk Symptoms (SOPS) or CAARMS but not both (SOPS only = 21, CAARMS only = 8, both SOPS and CAARMS = 1; BPRS only = 1), we z-transformed the SOPS positive symptom scales and CAARMS positive symptom scales (the most comparable subscales among others) using the mean and standard deviation of the whole CHR SOPS group and the whole CHR CAARMS group, respectively. We then tested associations between brain metrics and these positive-symptom z-scores using the combined SOPS and CAARMS samples. We further tested the associations for participants assessed using SOPS, due to the larger sample size.

For clinical symptom analysis, multiple comparison correction using false discovery rate (FDR) method [89] was applied across 7 SOPS domains or 4 CAARMS domains. For brain metrics, FDR correction was applied across global measures (4 measures) or network-level communities ($n = 9$).

RESULTS

A less efficient network configuration in CHR

On average, CHR individuals exhibited lower covariance strength than controls (FDR-corrected p , denoted as $q < 0.001$, Cohen's $d = 0.164$, see Fig. 2A and eTable 8). CHR also showed a less efficient global network configuration compared to controls, with lower global efficiency ($q = 0.027$, $d = 0.100$) and lower clustering coefficient ($q = 0.027$, $d = 0.087$) (Fig. 2B and eTable 8). Small worldness did not differ between CHR and controls (eTable 8). Global differences remained after controlling for antipsychotic exposure and were stable in the LOO site-effect sensitivity test (eResults 4 and 5) and the lateralisation-effect test (eResult 6 and eTable 16).

Among subgroups (eResults 3), BIPS showed lower small-worldness than non-BIPS and controls, while APS had higher small-worldness than non-APS. No differences were found in GRD subgroups or between APS and controls. These subgroup results were unaffected by antipsychotic exposure or site effects.

Frontotemporal network distinctiveness differences between CHR-T and CHR-NT

We detected nine network-level communities (Fig. 3A, eResult 2 and eTable 10). Given that one of the community structure identification criteria was similarity to the intrinsic networks [46], community grouping largely followed intrinsic networks, though

not identically due to large Desikan atlas regions. Subcortical regions were grouped within the same community. CT and SA metrics from the visual were grouped together and CT and SA metrics from the motor were in the same community. In contrast, CT and SA metrics from frontal and temporal regions were grouped according to morphometric types.

CHR-T exhibited higher temporal and frontal system segregation index (i.e., greater network distinctiveness) of SA communities than CHR-NT (temporal $q < 0.001$, $ES = 0.237$; frontal $q < 0.001$, $ES = 0.223$) and controls (temporal $q < 0.001$, $ES = 0.219$; frontal $q < 0.001$, $ES = 0.218$) (Fig. 3B). No significant difference was observed between CHR-NT and controls (eTable 9). In contrast, CHR-T had lower frontal CT community system segregation index than CHR-NT ($q < 0.001$, $ES = 0.208$) and controls ($q = 0.004$, $ES = 0.165$), with no differences between CHR-NT and controls (Fig. 3B).

Group differences in these communities remained significant after controlling for within-community mean SA or CT (eTable 9). Frontal SA or CT community differences persisted after controlling for antipsychotic exposure and were stable in LOO site-effect sensitivity tests (eResult 4) and the lateralisation-effect test (eResult 6 and eTable 16).

Within-network connectivity in temporal SA and frontal SA communities was higher in CHR-T than CHR-NT (temporal $q < 0.001$, $ES = 0.092$; frontal $q < 0.001$, $ES = 0.097$) and controls (temporal $q = 0.002$, $ES = 0.195$; frontal $q = 0.004$, $ES = 0.173$) (eTable 9). In contrast, within-network connectivity in frontal CT network was lower in CHR-T than CHR-NT ($q = 0.011$, $ES = 0.099$) and controls ($q < 0.001$, $ES = 0.211$). Between-community covariance did not significantly differ between CHR-T and CHR-NT.

These results suggest that the higher network distinctiveness of frontal and temporal surface area communities in CHR-T was driven by higher within-community covariance, not between-community alterations (eFigure 6). Similarly, the lower network distinctiveness of the frontal CT community in CHR-T was due to lower within-community covariance (eFigure 6).

Among the subgroups (eResult), no differences were found between APS and non-APS, or GRD and non-GRD groups. Interestingly, similar to transition-related difference, BIPS showed higher system segregation index in frontal and temporal SA communities than non-BIPS and controls. BIPS individuals had a higher percentage of CHR-T (31.9% of 71 BIPS) compared to APS (16.5%) or GRD (20.9%).

Relationship between network distinctiveness and clinical symptoms

No global network configuration measures were associated with clinical symptom severity. Instead, symptom associations were observed at the network level (eTable 11 and 12).

Using positive symptom z-scores from sites using SOPS or CAARMS, we found a significant interaction between transition status and the frontal SA community system segregation index ($p = 0.038$, only positive symptom z-scores were combined and thus no correction applied). Post-hoc analysis revealed that a greater frontal SA segregation index was associated with higher positive symptom z-scores in CHR-NT ($p = 0.004$), but not in CHR-T ($p = 0.177$).

This was replicated in sites using SOPS alone (interaction uncorrected $p = 0.018$, $q = 0.071$, eTable 11). Specifically, greater frontal SA community system segregation index was associated with greater SOPS positive symptoms in CHR-NT ($q = 0.008$), but not in CHR-T ($q = 0.536$) (eTable 12, Fig. 4, top row).

Moreover, a significant interaction between transition status and the frontal CT community segregation index was found for SOPS negative symptoms ($q = 0.032$, eTable 11). Post-hoc analysis revealed that lower frontal CT community system segregation index was associated with more severe SOPS negative symptoms in CHR-T (uncorrected $p = 0.016$, $q = 0.063$, Fig. 4 bottom row), but not in CHR-NT ($q = 0.806$, eTable 12).

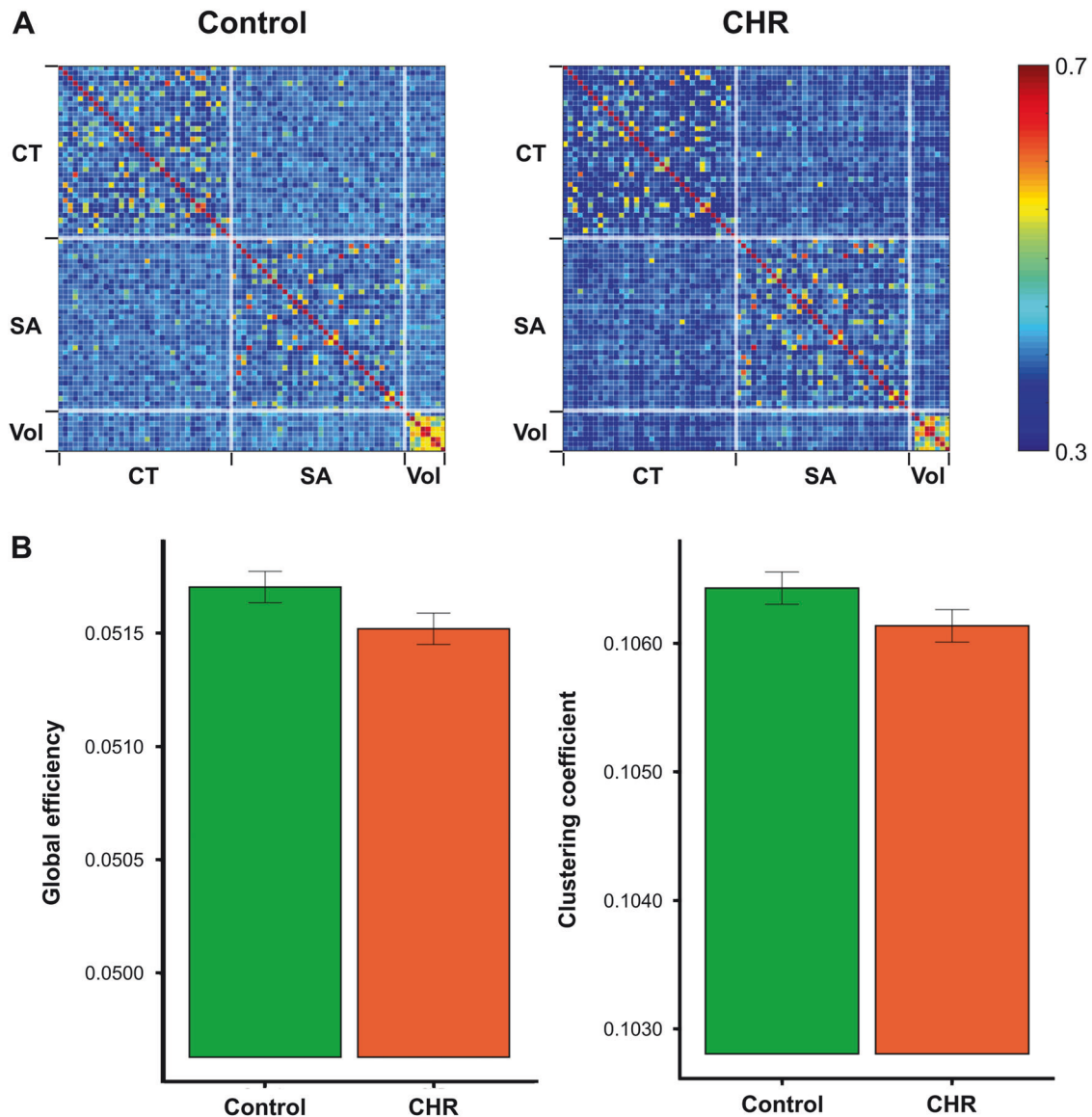


Fig. 2 A less efficient network configuration in CHR. **A** mean structural covariance matrix for healthy controls (left) and CHR individuals (right). Rows and columns follow the same order of 76 nodes (top to bottom and left to right). The colours indicate the covariance strength, with the lowest in blue and the highest in red. The white gridlines separate CT, SA and volume nodes. CHR individuals exhibited lower structural covariance than controls. **B** Bar charts (with standard errors) indicating lower global efficiency, local efficiency, and clustering coefficient in CHR individuals. CHR clinical high risk; CT cortical thickness; SA cortical surface area; Vol subcortical volume.

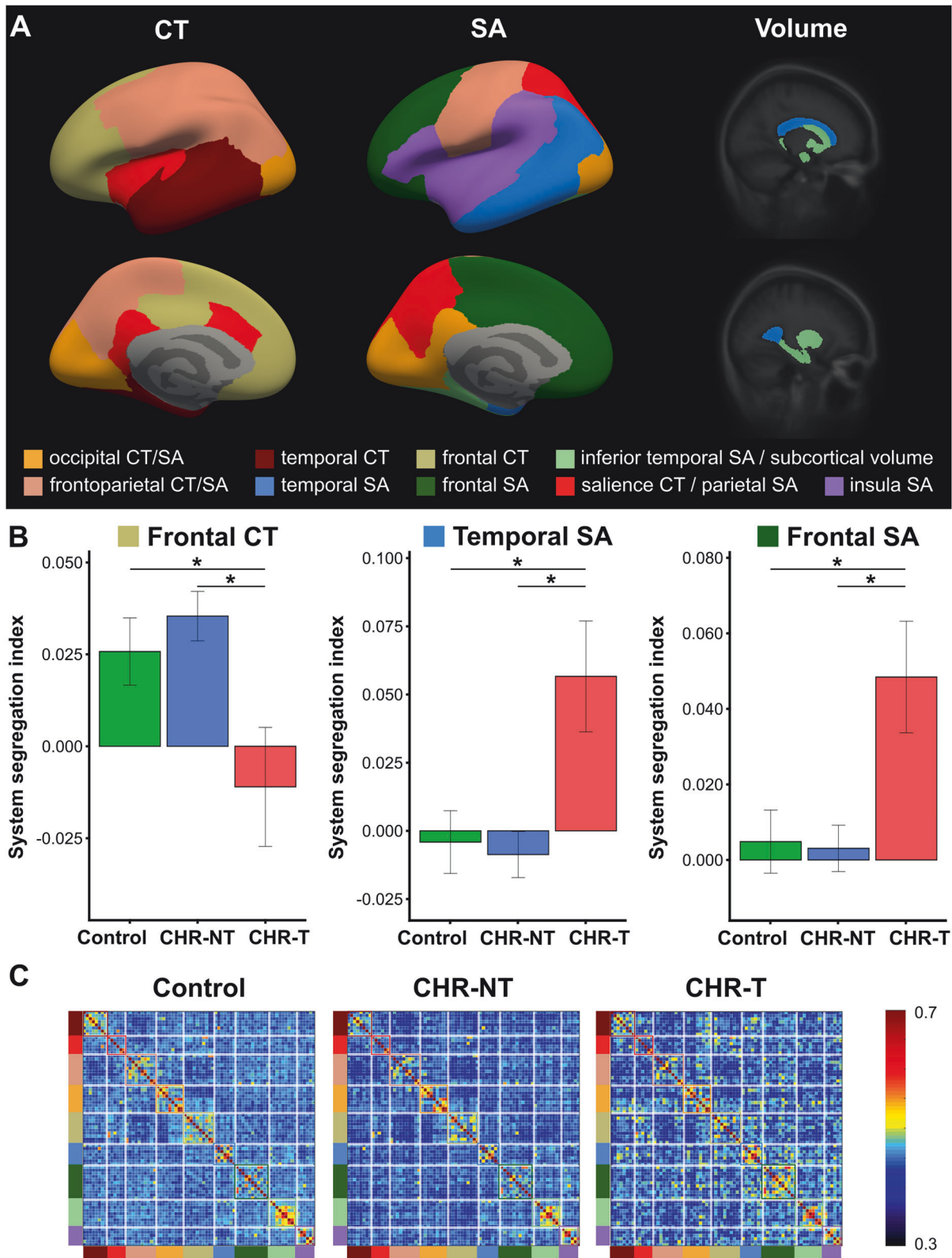
DISCUSSION

To better understand network-level alterations in CHR for psychosis, we investigated structural covariance networks and their symptom associations in a large CHR sample, yielding three key findings: First, at the global level, CHR individuals exhibited lower structural covariance and a less optimal structural network configuration than controls (i.e., lower global efficiency and lower clustering coefficient), with BIPS individuals showing lower small-worldness than non-BIPS individuals or controls. Second, CHR-T and CHR-NT differed only in frontotemporal network distinctiveness, not global metrics. This distinctiveness also separated BIPS from non-BIPS but not APS or GRD subgroups. Third, network-level metrics were associated with symptom severity in a transition-status-dependent manner: lower system segregation indices in the frontal SA network were related to lower positive symptoms in CHR-NT, while lower system segregation indices in the frontal CT network were related to higher negative symptoms in CHR-T.

These findings highlight the role of network topography in psychosis transition.

Structural network configuration in CHR is less coordinated and suboptimal

As expected, CHR individuals differed from healthy controls in global network configuration. These findings align with prior research from the ENIGMA CHR-P Workgroup, which reported subtle yet widespread structural differences [13], deviations from normative values [15], and greater anatomical deviance at the individual level [14] in CHR. In this study, the lower structure covariance in CHR might reflect reduced primary synaptic connections due to perinatal neurodevelopmental insults [90]. Without adequate protective effects from the primary connections, synaptic connections may suffer during pruning and result in a lower survival rate, leading to lower structural covariance.



Despite preserved integration-segregation balance (i.e., no small-worldness differences), CHR individuals exhibited a less optimal global network configuration than controls, as indicated by lower global efficiency and clustering coefficient. Lower global efficiency implies lower global communication capacity, while lower clustering coefficient indicates that network neighbours

were less likely to form clusters for efficient local processing [91–93]. Interestingly, two recent studies [40, 94] showed that individuals with schizophrenia could be vulnerable to nodal attack. Qualifying nodes into different types based on how well connected they were, Palaniyappan and colleagues [40] demonstrated that structural covariance networks in schizophrenia were

Fig. 3 Network distinctiveness was higher in frontal and temporal SA communities and lower in a frontal CT community in CHR-T versus CHR-NT. A Nine identified communities (colours) projected to surface (cortical regions) or structural image (subcortical regions). Among others, SA and CT of occipital and sensorimotor areas, and subcortical brain volumes, were grouped together into the same communities. Separate SA and CT communities were identified for temporal and frontal regions. **B** Bar charts (with standard errors) visualizing higher frontal and temporal SA system segregation index, and lower frontal CT community segregation index in CHR-T versus CHR-NT (FDR-corrected across 9 communities). Horizontal bar with * indicates significant group difference after FDR correction ($q < 0.05$). **C** mean structural covariance matrix for healthy controls (left), CHR-NT (middle) and CHR-T individuals (right). Rows and columns were grouped according to the 9 communities. The colour bars on the left and the bottom of each matrix and the colour boxes along the diagonal of each matrix indicate the community following the same colour scheme in Fig. 3A. Within each matrix, the colours indicate the covariance strength, with the lowest in blue and the highest in red. CHR-T individuals at clinical high risk for psychosis who transitioned to psychosis later in the follow-up; CHR-NT individuals at clinical high risk for psychosis who did not transition to psychosis later in the follow-up; CT cortical thickness; SA cortical surface area; q FDR corrected p value; FDR false discovery rate.

particularly sensitive to hub (the highly connected nodes) removal. Future studies should examine whether CHR individuals exhibit similar vulnerabilities due to their suboptimal network configuration.

Frontotemporal network deviation from typical development

CHR-T individuals exhibited greater network distinctiveness in the frontal and temporal SA networks and lower distinctiveness in the frontal CT network compared to CHR-NT and controls. CHR-T individuals also had more severe positive and negative symptoms than CHR-NT. Given the study-specific control groups well matched with the CHR individuals on both site effects and participant backgrounds, such differences indicated deviations from typical development rather than merely normal individual variability. Importantly, across all three frontotemporal networks, CHR-T participants deviated from controls in the same direction as from CHR-NT, while CHR-NT did not differ from controls. Lifespan studies [95] showed that early life to young adulthood is dominated by greater global integration and reduced segregation. From adolescence to young adulthood, the frontoparietal and dorsal attention networks undergo increased between-network covariance and decreased within-network covariance [96]. In our study, network distinctiveness differences were driven by altered within-network covariance, suggesting frontotemporal developmental trajectory deviations from typical development may be linked to a higher transition risk in CHR.

Though both CT- and SA-based frontal network distinctiveness deviated from typical development in CHR-T, the deviations were in opposite directions. CT and SA have distinct genetics [70, 71], neurobiology [72–75], and maturation trajectories [76, 77]. Genetically, CT is linked to post-mid-fetal processes including branching, synaptic pruning and myelination, while SA are related to moderation of fetal neurogenesis [70]. Mechanically, in prenatal and perinatal development, CT reflects cellular density within radial units [72, 77], whereas SA is tied to radial unit density and neuron migration [72, 97]. From childhood to adolescence, a combination of normal neurodevelopmental mechanisms including synaptogenesis, gliogenesis, dendritic arborization, and intracortical myelination facilitate CT and SA changes [72–75]. Further, adolescence is a time when CT declines faster than SA [77], which coincides with large CT difference between CHR and controls than SA [13]. Frontal network differences could therefore be driven by a combination of neurodevelopmental differences and pathological processes [98]. Pathologically, CT changes can reflect abnormal synaptic plasticity [99, 100], neuroinflammation [101, 102], oxidative stress [103, 104], and neurotransmitter dysfunction [105]. Elevated free water, a marker of neuroinflammation, appears in first-episode psychosis but not CHR, indicating inflammation peaks around transition [106, 107]. Further research is needed to link frontal structural networks to specific pathologies [108].

Cortical thickness and surface area network distinctiveness: links to symptoms and transition

CHR-T individuals had more severe positive symptoms than CHR-NT, consistent with their higher risk of developing psychosis. As a

group, CHR-T individuals also showed higher network distinctiveness in the frontal and temporal SA networks than CHR-NT and control individuals. These group differences implied that the frontotemporal SA network distinctiveness deviating from typical development may be related to positive symptom severity. This is further supported by findings in CHR-NT, where higher frontal SA network distinctiveness was associated with more severe positive symptoms. Notably, threshold positive symptom constitutes psychosis diagnosis, and CHR-T individuals eventually transitioned to psychosis during follow-up. These results suggested that atypical frontal SA network distinctiveness was associated with worsening symptoms in CHR until transition is imminent. At that point, frontal SA network distinctiveness may shift from increasing to decreasing due to the progression of atrophy from stage 2 to stage 3 (see *The network hypothesis of schizophrenia*), thereby losing its positive association with symptom severity in the CHR-T group.

Conversely, CHR-T individuals had more severe negative symptoms and less distinct frontal CT network than CHR-NT individuals. These group differences implied that the frontal CT network distinctiveness deviating from typical development may be related to negative symptom severity. This is further supported by findings in CHR-T, where lower frontal CT network distinctiveness was related to higher negative symptoms, an association absent in CHR-NT. This suggests that frontal CT network deviations emerge closer to psychosis onset (stage 1 in atrophy progression, see *The network hypothesis of schizophrenia*).

The network hypothesis of schizophrenia

The divergent transition-related frontal SA and CT network alterations in CHR-NT and CHR-T may reflect the different network breakdown stages (Fig. 5). The network-based spreading hypothesis states that structural deficits propagate to distant regions that are strongly connected with the initial regions [54–56]. Disruption of signalling, trophic support, and neurotransmitter system due to initial focal deficit can affect neuronal survival of the distal connected regions [57]. Hens and colleagues [61, 109] demonstrated that signal propagation was governed by path lengths, typically shorter within than between networks, translating network topology into predicted dynamic outcomes. Further, the human brain has small-world [110] and modular architecture [38] that stays robust to random focal atrophy [63] and buffers the atrophy from immediately spreading to multi-networks [64, 65]. Consequently, the signal propagation across networks follows a step-like pattern reflecting the discrete nature of cross-network advancements [61]. In this context, structural deficit propagation can be divided into three stages (Fig. 5A and see further detailed discussion in the supplementary): Stage one where focal structural deficits disturb the within-network covariance and lower the network distinctiveness; stage two where pathology dominates the within-network covariance and heightens the network distinctiveness; and stage three structural deficits spread to more networks resulting in lower network distinctiveness.

The lower frontal CT network distinctiveness and the association with clinical symptoms in CHR-T—but not CHR-NT

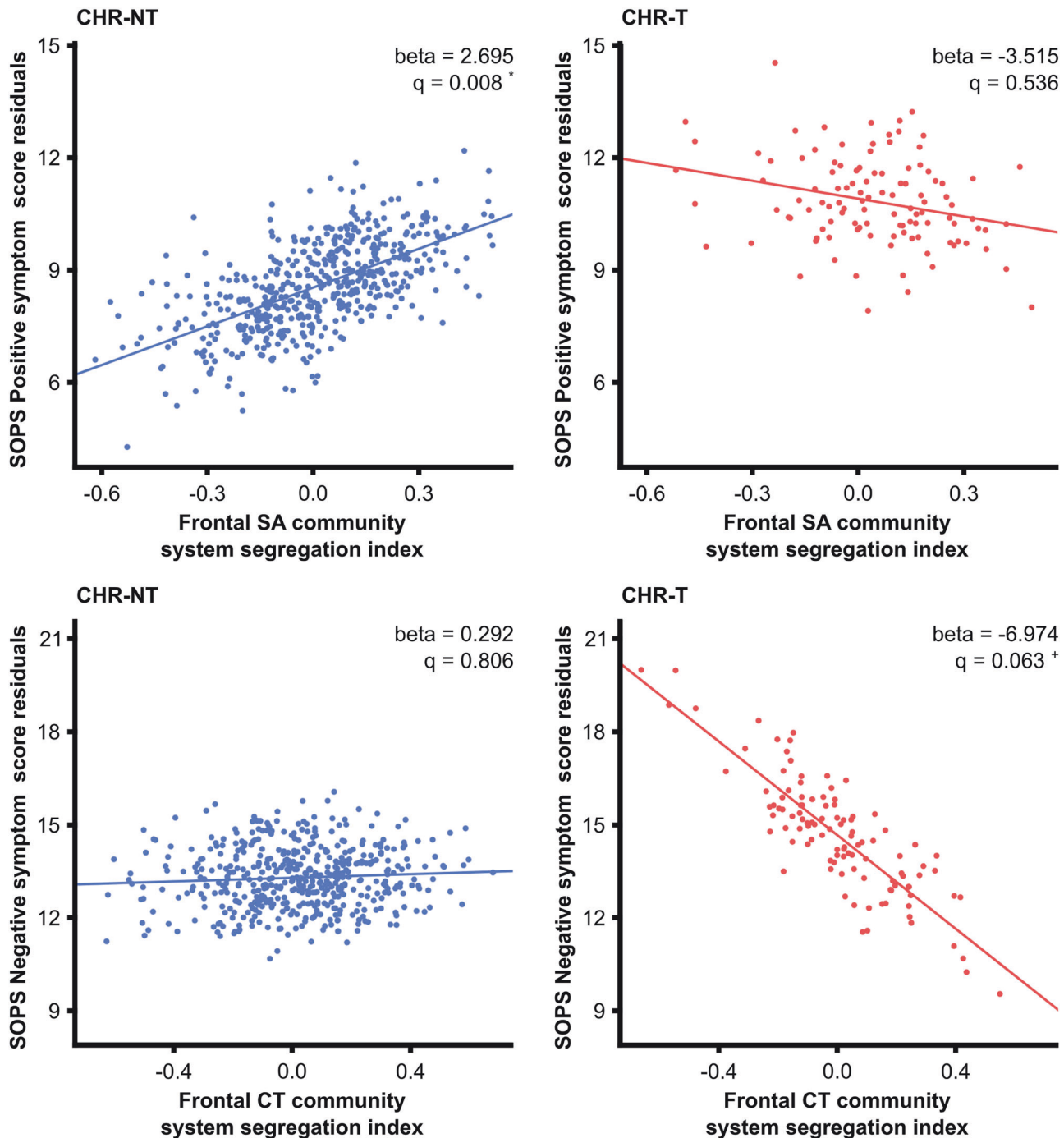
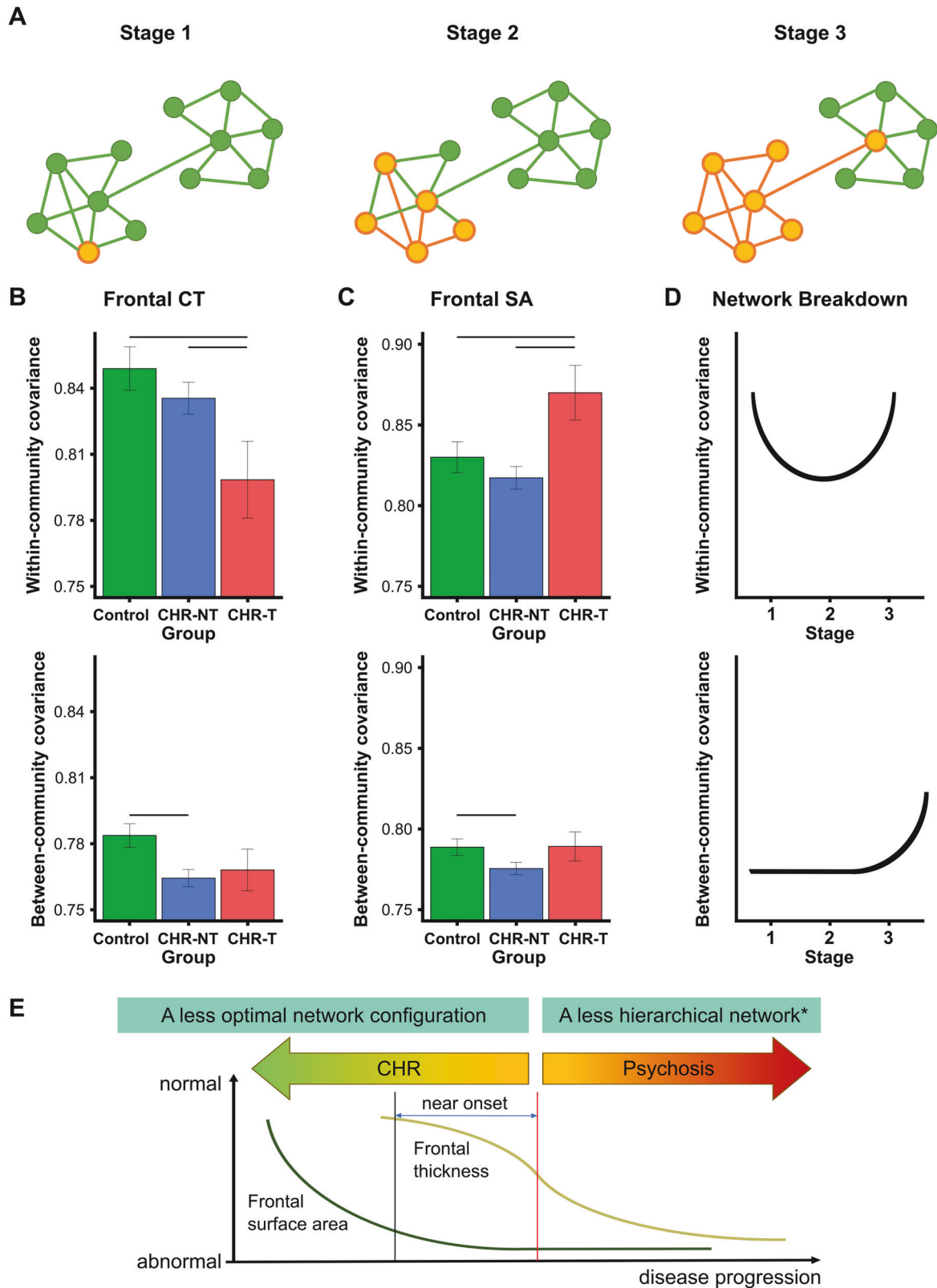


Fig. 4 Association between network distinctiveness and clinical symptoms. Residuals, after removing the effects of age, sex and random intercepts of site from the clinical scores estimated using the LMM method, were plotted against the system segregation index of the frontal communities. Each dot represents one participant. The lines indicate the fitted association. The beta and p values were estimated using the LMM method before FDR correction. **Upper panel:** Higher frontal SA community system segregation index was associated with higher SOPS positive symptom score in CHR-NT ($q = 0.008$). CHR-T was higher in frontal SA system segregation index and SOPS positive symptom score than CHR-NT. **Lower panel:** The lower frontal CT community was associated with higher SOPS negative symptom scores in CHR-T (uncorrected $p = 0.016$, $q = 0.063$). CHR-T was lower in the frontal CT community system segregation index and higher in SOPS negative symptom scores than CHR-NT. CHR-T individuals at clinical high risk for psychosis who transitioned to psychosis later in the follow-up; CHR-NT individuals at clinical high risk for psychosis who did not transit to psychosis later in the follow-up; SA cortical surface area; CT cortical thickness; SOPS Scale of Psychosis-risk Symptoms; LMM linear mixed modelling; q FDR corrected p value; FDR false discovery rate; * significant at both uncorrected $p < 0.05$ and corrected $p < 0.05$; + significant at uncorrected $p < 0.05$ but did not survive multiple comparison corrections.

may reflect the first stage of the network's breakdown (Fig. 5A and B). CHR-T individuals, who transitioned to psychosis during follow-up, may experience pathological processes atop pre-existing CHR-related abnormalities, disrupting frontal CT

network covariation (Fig. 5B upper) while sparing its connectivity with the rest of the brain (Fig. 5B lower). In contrast, increased frontal and temporal SA network distinctiveness, driven by higher within-network covariance, suggests these



networks belong to a second stage (Fig. 5A, C). Frontal SA abnormalities in CHR are limited to 8 of 68 regions [13], and covariance with the rest of the brain remains intact (Fig. 5C lower), indicating it has not yet reached the third stage.

We expect psychosis onset with cascading effects that would result in multinet network failures due to pathological signal spillover. Psychosis onset is expected when between-network covariance is affected. Previous studies suggest schizophrenia networks are less

Fig. 5 Schematic representations of network breakdown stages. **A** Schematic representations of deficits spreading from stage 1 to 3 of network breakdown. Circles represent nodes in the network. Lines connecting the circles are edges in the network. Two networks are depicted where deficits (orange circle) spread from one network (left) to the other (right). Orange lines indicate the path of spreading from the initial deficit node in stage 1, followed by the spreading to four additional nodes within the network (left) in stage 2, and eventually affecting node of the other network (right) in stage 3. **B** Within (upper panel) and between (lower panel) network covariance of the frontal CT network. We interpreted the lower frontal CT network distinctiveness in CHR-T than CHR-NT to reflect stage 1 of the frontal CT's network breakdown, which is driven by the lower within-network covariance (upper panel). **C** Within (upper panel) and between (lower panel) network covariance of the frontal SA network. We interpreted the higher frontal SA network distinctiveness in CHR-T than CHR-NT to reflect stage 2 of the frontal SA's network breakdown, which is driven by the higher within-network covariance (upper panel). In **B** and **C**, lower between-network covariance in CHR-NT than controls may reflect the lower mean structural covariance in CHR than controls. Horizontal bars indicate significant group differences ($q < 0.05$). **D** Schematic representations of within (upper panel) and between (lower panel) network covariance changes across network breakdown stages. We expect that the stage 1 and 2 of network breakdown are dominated by within-network covariance changes. The between-network covariance increase in stage 3 due to deficit spreading across communities. **E** A schematic summary of the network breakdown stages. * based on the literature [22]. CHR-T individuals at clinical high risk for psychosis who transitioned to psychosis later in the follow-up; CHR-NT individuals at clinical high risk for psychosis who did not transit to psychosis later in the follow-up; CT cortical thickness; SA cortical surface area; q FDR corrected p value; FDR false discovery rate.

hierarchical and experience hyper-covariations compared to controls [36, 111, 112]. Though the CHR individuals in this study are in clinical stage one that is based on symptoms and functioning [113–115], brain networks exhibit different breakdown stages, highlighting neuroimaging network markers as early indicators of disorder progression.

Limitations and conclusions

Our study has several limitations. First, the findings are based on cross-sectional T1 structural data, while the network-based spreading hypothesis is inherently longitudinal. Longitudinal datasets are necessary to better characterize brain network changes across CHR stages and transitions to psychosis. Second, due to inter-site assessment differences, we could not assess the relationship between subsyndrome-related brain alterations and symptoms or use a larger sample for brain-symptom associations. Future studies with more homogeneous assessment tools [116] across sites are needed. Third, the ENIGMA cohort is pooled from existing studies from various sites. While we controlled for antipsychotic use, we lacked data on medication dose and duration. Lastly, due to the IRB constraints on data sharing from different sites, we do not have access to voxel/vertex level data. Research using finer brain parcellation and voxel/vertex level structural data could provide more sensitive and robust metrics for detect early changes [117, 118] and the possible lateralisation effects in CHR.

In conclusion, CHR individuals exhibit lower structural covariance and less optimal structural network configuration than controls. Greater frontotemporal SA network distinctiveness may indicate SA abnormality, even without transition to psychosis, with the frontal SA network linked to positive symptoms. Conversely, a less distinctive frontal CT network was associated with negative symptoms among those who later transitioned, suggesting additional transition-related mechanisms. These findings support the network-based spreading hypothesis, highlighting the value of network topography in understanding psychosis progression.

DATA AVAILABILITY

Currently, regional-level data are available upon reasonable request pending appropriate study approvals and data transfer agreements between participating institutions (see <https://enigma.ini.usc.edu/ongoing/enigma-clinical-high-risk/>). Interested researchers should contact Maria Jalbrzikowski (Maria.Jalbrzikowski@childrens.harvard.edu) and Dennis Hernaes (dennis.hernaes@maastrichtuniversity.nl).

CODE AVAILABILITY

Codes used in this manuscript are available at https://github.com/hzlab/2025Liu_MP_ENIGMA_CHR_SCN.

REFERENCES

1. Yung AR, McGorry PD, McFarlane CA, Jackson HJ, Patton GC, Rakkar A. Monitoring and care of young people at incipient risk of psychosis. *Schizophr Bull.* 1996;22:283–303.
2. Salazar de Pablo G, Radua J, Pereira J, Bonoldi I, Arienti V, Besana F, et al. Probability of transition to psychosis in individuals at clinical high risk: an updated meta-analysis. *JAMA Psychiatry.* 2021;78:970–8.
3. Fusar-Poli P, Bonoldi I, Yung AR, Borgwardt S, Kempton MJ, Valmaggia L, et al. Predicting psychosis: meta-analysis of transition outcomes in individuals at high clinical risk. *Arch Gen Psychiatry.* 2012;69:220–9.
4. McGlashan TH, Walsh BC, Woods SW, Addington J, Cadenhead K, Cannon T, et al. Structured interview for psychosis-risk syndromes. New Haven, CT: Yale School of Medicine. 2001.
5. Yung AR, Yung AR, Pan Yuen H, McGorry PD, Phillips LJ, Kelly D, et al. Mapping the onset of psychosis: the comprehensive assessment of at-risk mental states. *Aust N Z J Psychiatry.* 2005;39:964–71.
6. Hui C, Morcillo C, Russo DA, Stochl J, Shelley GF, Painter M, et al. Psychiatric morbidity, functioning and quality of life in young people at clinical high risk for psychosis. *Schizophr Res.* 2013;148:175–80.
7. Kelleher I, Murtagh A, Molloy C, Roddy S, Clarke MC, Harley M, et al. Identification and characterization of prodromal risk syndromes in young adolescents in the community: a population-based clinical interview study. *Schizophr Bull.* 2012;38:239–46.
8. Granö N, Karjalainen M, Edlund V, Saari E, Itkonen A, Anto J, et al. Health-related quality of life among adolescents: a comparison between subjects at risk for psychosis and other help seekers. *Early Interv Psychiatry.* 2014;8:163–9.
9. Ruhrmann S, Paruch J, Bechdolf A, Pukrop R, Wagner M, Berning J, et al. Reduced subjective quality of life in persons at risk for psychosis. *Acta Psychiatr Scand.* 2008;117:357–68.
10. Fusar-Poli P, Estradé A, Stanghellini G, Venables J, Onumere J, Messas G, et al. The lived experience of psychosis: a bottom-up review co-written by experts by experience and academics. *World Psychiatry.* 2022;21:168–88.
11. Fusar-Poli P, Davies C, Solmi M, Brondino N, De Micheli A, Kotlicka-Antczak M, et al. Preventive treatments for psychosis: Umbrella review (Just the Evidence). *Front Psychiatry.* 2019;10:764.
12. Fusar-Poli P, Correll CU, Arango C, Berk M, Patel V, Ioannidis JPA. Preventive psychiatry: a blueprint for improving the mental health of young people. *World Psychiatry.* 2021;20:200–21.
13. Jalbrzikowski M, Hayes RA, Wood SJ, Nordholm D, Zhou JH, Fusar-Poli P, et al. Association of structural magnetic resonance imaging measures with psychosis onset in individuals at clinical high risk for developing psychosis. *JAMA Psychiatry.* 2021;78:1–14.
14. Baldwin H, Radua J, Antoniadis M, Haas SS, Frangou S, Agartz I, et al. Neuroanatomical heterogeneity and homogeneity in individuals at clinical high risk for psychosis. *Transl Psychiatry.* 2022;12:1–11.
15. Haas SS, Ge R, Agartz I, Amminger GP, Andreassen OA, Bachman P, et al. Normative Modeling of Brain Morphometry in Clinical High Risk for Psychosis. *JAMA Psychiatry.* 2024;81:77–88.
16. van Erp TGM, Walton E, Hibar DP, Schmaal L, Jiang W, Glahn DC, et al. Cortical brain abnormalities in 4474 individuals with schizophrenia and 5098 controls via the ENIGMA consortium. *Biol Psychiatry.* 2018;84:644–54.
17. van Erp TGM, Hibar DP, Rasmussen JM, Glahn DC, Pearlson GD, Andreassen OA, et al. Subcortical brain volume abnormalities in 2028 individuals with schizophrenia and 2540 healthy controls via the ENIGMA consortium. *Mol Psychiatry.* 2016;21:547–53.

18. Zhu Y, Maikusa N, Radua J, Sámann PG, Fusar-Poli P, Agartz I, et al. Using brain structural neuroimaging measures to predict psychosis onset for individuals at clinical high-risk. *Mol Psychiatry*. 2024;29:1465–77.
19. Collins MA, Ji JL, Chung Y, Lympus CA, Afriyie-Agyemang Y, Addington JM, et al. Accelerated cortical thinning precedes and predicts conversion to psychosis: The NAPLS3 longitudinal study of youth at clinical high-risk. *Mol Psychiatry*. 2023;28:1182–9.
20. Chung Y, Allswede D, Addington J, Bearden CE, Cadenhead K, Cornblatt B, et al. Cortical abnormalities in youth at clinical high-risk for psychosis: findings from the NAPLS2 cohort. *Neuroimage Clin*. 2019;23:101862.
21. Pantelis C, Velakoulis D, McGorry PD, Wood SJ, Suckling J, Phillips LJ, et al. Neuroanatomical abnormalities before and after onset of psychosis: a cross-sectional and longitudinal MRI comparison. *Lancet*. 2003;361:281–8.
22. Doucet GE, Lin D, Du Y, Fu Z, Glahn DC, Calhoun VD, et al. Personalized estimates of morphometric similarity in bipolar disorder and schizophrenia. *NPJ Schizophr*. 2020;6:39.
23. Prasad K, Rubin J, Mitra A, Lewis M, Theis N, Muldoon B, et al. Structural covariance networks in schizophrenia: a systematic review Part II. *Schizophr Res*. 2022;239:176–91.
24. Kim S, Kim Y-W, Jeon H, Im C-H, Lee S-H. Altered cortical thickness-based individualized structural covariance networks in patients with schizophrenia and bipolar disorder. *J Clin Med*. 2020;9:1846.
25. Niu L, Fang K, Han S, Xu C, Sun X. Resolving heterogeneity in schizophrenia, bipolar I disorder, and attention-deficit/hyperactivity disorder through individualized structural covariance network analysis. *Cereb Cortex*. 2024;34:bhad391.
26. Alexander-Bloch A, Giedd JN, Bullmore E. Imaging structural co-variance between human brain regions. *Nat Rev Neurosci*. 2013;14:322–36.
27. Sebenius I, Dorfschmidt L, Seidlitz J, Alexander-Bloch A, Morgan SE, Bullmore E. Structural MRI of brain similarity networks. *Nat Rev Neurosci*. 2025;26:42–59.
28. Alexander-Bloch A, Raznahan A, Bullmore E, Giedd J. The convergence of maturational change and structural covariance in human cortical networks. *J Neurosci*. 2013;33:2889–99.
29. Khundrakpam BS, Lewis JD, Jeon S, Kostopoulos P, Itturia Medina Y, Chouinard-Decorte F, et al. Exploring individual brain variability during development based on patterns of maturational coupling of cortical thickness: a longitudinal MRI study. *Cereb Cortex*. 2019;29:178–88.
30. Segall JM, Allen EA, Jung RE, Erhardt EB, Arja SK, Kiehl K, et al. Correspondence between structure and function in the human brain at rest. *Front Neuroinform*. 2012;6:10.
31. Seeley WW, Crawford RK, Zhou J, Miller BL, Greicius MD. Neurodegenerative diseases target large-scale human brain networks. *Neuron*. 2009;62:42–52.
32. Hunt BAE, Tewarie PK, Mougín OE, Geades N, Jones DK, Singh KD, et al. Relationships between cortical myeloarchitecture and electrophysiological networks. *Proc Natl Acad Sci*. 2016;113:13510–5.
33. Yee Y, Fernandes DJ, French L, Ellegood J, Cahill LS, Vousden DA, et al. Structural covariance of brain region volumes is associated with both structural connectivity and transcriptomic similarity. *Neuroimage*. 2018;179:357–72.
34. Prasad K, Rubin J, Mitra A, Lewis M, Theis N, Muldoon B, et al. Structural covariance networks in schizophrenia: a systematic review Part I. *Schizophr Res*. 2022;240:1–21.
35. Watts DJ, Strogatz SH. Collective dynamics of 'small-world' networks. *Nature*. 1998;393:440–2.
36. Bassett DS, Bullmore E, Verchinski BA, Mattay VS, Weinberger DR, Meyer-Lindenberg A. Hierarchical Organization of Human Cortical Networks in Health and Schizophrenia. *J Neurosci*. 2008;28:9239–48.
37. Baum GL, Ciric R, Roalf DR, Betzel RF, Moore TM, Shinohara RT, et al. Modular segregation of structural brain networks supports the development of executive function in youth. *Curr Biol*. 2017;27:1561–72.e8.
38. Meunier D, Lambiotte R, Bullmore ET. Modular and hierarchically modular organization of brain networks. *Front Neurosci*. 2010;4:200.
39. Chan MY, Park DC, Savalia NK, Petersen SE, Wig GS. Decreased segregation of brain systems across the healthy adult lifespan. *PNAS*. 2014;111:E4997–E5006.
40. Palaniyappan L, Hodgson O, Balain V, Iwabuchi S, Gowland P, Liddle P. Structural covariance and cortical reorganisation in schizophrenia: a MRI-based morphometric study. *Psychol Med*. 2019;49:412–20.
41. Zhang Y, Lin L, Lin C-P, Zhou Y, Chou K-H, Lo C-Y, et al. Abnormal topological organization of structural brain networks in schizophrenia. *Schizophr Res*. 2012;141:109–18.
42. Nelson EA, White DM, Kraguljac NV, Lahti AC. Gyrfication connectomes in unmedicated patients with schizophrenia and following a short course of antipsychotic drug treatment. *Front Psychiatry*. 2018;9:699.
43. Palaniyappan L, Park B, Balain V, Dangi R, Liddle P. Abnormalities in structural covariance of cortical gyrfication in schizophrenia. *Brain Struct Funct*. 2015;220:2059–71.
44. Liu F, Tian H, Li J, Li S, Zhuo C. Altered voxel-wise gray matter structural brain networks in schizophrenia: association with brain genetic expression pattern. *Brain Imaging Behav*. 2019;13:493–502.
45. Zugman A, Assunção I, Vieira G, Gadelha A, White TP, Oliveira PPM, et al. Structural covariance in schizophrenia and first-episode psychosis: an approach based on graph analysis. *J Psychiatr Res*. 2015;71:89–96.
46. Drakesmith M, Caeyenberghs K, Dutt A, Zammit S, Evans CJ, Reichenberg A, et al. Schizophrenia-like topological changes in the structural connectome of individuals with subclinical psychotic experiences. *Hum Brain Mapp*. 2015;36:2629–43.
47. Sandini C, Scariati E, Padula MC, Schneider M, Schaer M, Van De Ville D, et al. Cortical dysconnectivity measured by structural covariance is associated with the presence of psychotic symptoms in 22q11.2 deletion syndrome. *Biol Psychiatry: Cogn Neurosci Neuroimaging*. 2018;3:433–42.
48. Das T, Borgwardt S, Hauke DJ, Harrisberger F, Lang UE, Riecher-Rössler A, et al. Disorganized gyrfication network properties during the transition to psychosis. *JAMA Psychiatry*. 2018;75:613–22.
49. Tijms BM, Sprooten E, Job D, Johnstone EC, Owens DGC, Willshaw D, et al. Grey matter network in people at increased familial risk for schizophrenia. *Schizophr Res*. 2015;168:1–8.
50. Zhang W, Lei D, Keedy SK, Ivleva EI, Eum S, Yao L, et al. Brain gray matter network organization in psychotic disorders. *Neuropsychopharmacology*. 2020;45:666–74.
51. Li X, Wu K, Zhang Y, Kong L, Bertisch H, DeLisi LE. Altered topological characteristics of morphological brain network relate to language impairment in high genetic risk subjects and schizophrenia patients. *Schizophr Res*. 2019;208:338–43.
52. Shi F, Yap P-T, Gao W, Lin W, Gilmore JH, Shen D. Altered structural connectivity in neonates at genetic risk for schizophrenia: a combined study using morphological and white matter networks. *Neuroimage*. 2012;62:1622–33.
53. Raj A. Graph models of pathology spread in Alzheimer's disease: an alternative to conventional graph theoretic analysis. *Brain Connect*. 2021;11:799–814.
54. Raj A, Powell F. Models of network spread and network degeneration in brain disorders. *Biol Psychiatry: Cogn Neurosci Neuroimaging*. 2018;3:788–97.
55. Wannan CMJ, Cropley VL, Chakravarty MM, Bousman C, Ganella EP, Bruggemann JM, et al. Evidence for network-based cortical thickness reductions in schizophrenia. *AJP*. 2019;176:552–63.
56. Chopra S, Segal A, Oldham S, Holmes A, Sabarodien K, Orchard ER, et al. Network-based spreading of gray matter changes across different stages of psychosis. *JAMA Psychiatry*. 2023. 20 September 2023. <https://doi.org/10.1001/jamapsychiatry.2023.3293>.
57. Vogel JW, Corriveau-Lecavalier N, Franzmeier N, Pereira JB, Brown JA, Maass A, et al. Connectome-based modelling of neurodegenerative diseases: towards precision medicine and mechanistic insight. *Nat Rev Neurosci*. 2023;24:620–39.
58. Shafiei G, Markello RD, Makowski C, Talpalari A, Kirschner M, Devenyi GA, et al. Spatial patterning of tissue volume loss in schizophrenia reflects brain network architecture. *Biol Psychiatry*. 2020;87:727–35.
59. von Economo CF, Koskinas GN Die cytoarchitektonik der hirnrinde des erwachsenen menschen. J. Springer; 1925.
60. Scholtens LH, de Reus MA, de Lange SC, Schmidt R, van den Heuvel MP. An MRI Von Economo – Koskinas atlas. *Neuroimage*. 2018;170:249–56.
61. Hens C, Harush U, Haber S, Cohen R, Barzel B. Spatiotemporal signal propagation in complex networks. *Nat Phys*. 2019;15:403–12.
62. Kaiser M, Martin R, Andras P, Young MP. Simulation of robustness against lesions of cortical networks. *Eur J Neurosci*. 2007;25:3185–92.
63. Gu S, Pasqualetti F, Cieslak M, Telesford QK, Yu AB, Kahn AE, et al. Controllability of structural brain networks. *Nat Commun*. 2015;6:8414.
64. Ewers M, Luan Y, Frontzkowski L, Neitzel J, Rubinski A, Dichgans M, et al. Segregation of functional networks is associated with cognitive resilience in Alzheimer's disease. *Brain*. 2021;144:2176–85.
65. Buldyrev SV, Parshani R, Paul G, Stanley HE, Havlin S. Catastrophic cascade of failures in interdependent networks. *Nature*. 2010;464:1025–8.
66. McGlashan T, Walsh B, Woods S, McGlashan T, Walsh B, Woods S. The Psychosis-Risk Syndrome: Handbook for Diagnosis and Follow-Up. Oxford, New York: Oxford University Press; 2010.
67. Desikan RS, Ségonne F, Fischl B, Quinn BT, Dickerson BC, Blacker D, et al. An automated labeling system for subdividing the human cerebral cortex on MRI scans into gyral based regions of interest. *Neuroimage*. 2006;31:968–80.
68. Radua J, Vieta E, Shinohara R, Kochunov P, Quidé Y, Green MJ, et al. Increased power by harmonizing structural MRI site differences with the ComBat batch adjustment method in ENIGMA. *Neuroimage*. 2020;218:116956.
69. Yun J-Y, Boedhoe PSW, Vriend C, Jahanshad N, Abe Y, Ameis SH, et al. Brain structural covariance networks in obsessive-compulsive disorder: a graph analysis from the ENIGMA Consortium. *Brain*. 2020;143:684–700.

70. Grasby KL, Jahanshad N, Painter JN, Colodro-Conde L, Bralten J, Hibar DP, et al. The genetic architecture of the human cerebral cortex. *Science*. 2020;367:eaay6690.
71. Palaniyappan L, Mallikarjun P, Joseph V, White TP, Liddle PF. Regional contraction of brain surface area involves three large-scale networks in schizophrenia. *Schizophr Res*. 2011;129:163–8.
72. Rakic P. Specification of cerebral cortical areas. *Science*. 1988;241:170–6.
73. Petanjek Z, Judaš M, Šimić G, Rašin MR, Uylings HBM, Rakic P, et al. Extraordinary neoteny of synaptic spines in the human prefrontal cortex. *Proc Natl Acad Sci USA*. 2011;108:13281–6.
74. Hill J, Inder T, Neil J, Dierker D, Harwell J, Van Essen D. Similar patterns of cortical expansion during human development and evolution. *Proc Natl Acad Sci USA*. 2010;107:13135–40.
75. Garcia KE, Kroenke CD, Bayly PV. Mechanics of cortical folding: stress, growth and stability. *Philos Trans R Soc Lond B Biol Sci*. 2018;373:20170321.
76. Bethlehem Ral, Seidlitz J, White SR, Vogel JW, Anderson KM, Adamson C, et al. Brain charts for the human lifespan. *Nature*. 2022;604:525–33.
77. Tamnes CK, Herting MM, Goddings A-L, Meuwese R, Blakemore S-J, Dahl RE, et al. Development of the cerebral cortex across adolescence: a multisample study of inter-related longitudinal changes in cortical volume, surface area, and thickness. *J Neurosci*. 2017;37:3402–12.
78. Muftuler LT, Davis EP, Buss C, Head K, Hasso AN, Sandman CA. Cortical and subcortical changes in typically developing preadolescent children. *Brain Res*. 2011;1399:15–24.
79. Sydnor VJ, Larsen B, Bassett DS, Alexander-Bloch A, Fair DA, Liston C, et al. Neurodevelopment of the association cortices: patterns, mechanisms, and implications for psychopathology. *Neuron*. 2021;109:2820–46.
80. Chen L, Wang Y, Wu Z, Shan Y, Li T, Hung S-C, et al. Four-dimensional mapping of dynamic longitudinal brain subcortical development and early learning functions in infants. *Nat Commun*. 2023;14:3727.
81. Sydnor VJ, Larsen B, Seidlitz J, Adebimpe A, Alexander-Bloch AF, Bassett DS, et al. Intrinsic activity development unfolds along a sensorimotor–association cortical axis in youth. *Nat Neurosci*. 2023;26:638–49.
82. Toro R, Perron M, Pike B, Richer L, Veillette S, Pausova Z, et al. Brain size and folding of the human cerebral cortex. *Cereb Cortex*. 2008;18:2352–7.
83. Fornito A, Zalesky A, Breakspear M. Graph analysis of the human connectome: promise, progress, and pitfalls. *Neuroimage*. 2013;80:426–44.
84. Yeo BTT, Krienen FM, Sepulcre J, Sabuncu MR, Lashkari D, Hollinshead M, et al. The organization of the human cerebral cortex estimated by intrinsic functional connectivity. *J Neurophysiol*. 2011;106:1125–65.
85. Lancichinetti A, Fortunato S. Consensus clustering in complex networks. *Sci Rep*. 2012;2:1–7.
86. Blondel VD, Guillaume J-L, Lambiotte R, Lefebvre E. Fast unfolding of communities in large networks. *J Stat Mech*. 2008;2008:P10008.
87. Rand WM. Objective criteria for the evaluation of clustering methods. *J Am Stat Assoc*. 1971;66:846–50.
88. Thomas DR, Rao JNK. Small-sample comparisons of level and power for simple goodness-of-fit statistics under cluster sampling. *J Am Stat Assoc*. 1987;82:630–6.
89. Benjamini Y, Hochberg Y. Controlling the false discovery rate: a practical and powerful approach to multiple testing. *J R Stat Soc: Series B (Methodological)*. 1995;57:289–300.
90. Bullmore ET, Woodruff PWR, Wright IC, Rabe-Hesketh S, Howard RJ, Shuriquie N, et al. Does dysplasia cause anatomical dysconnectivity in schizophrenia? *Schizophr Res*. 1998;30:127–35.
91. Bassett DS, Bullmore ET. Human brain networks in health and disease. *Curr Opin Neurol*. 2009;22:340–7.
92. Lynall M-E, Bassett DS, Kerwin R, McKenna PJ, Kitzbichler M, Muller U, et al. Functional connectivity and brain networks in schizophrenia. *J Neurosci*. 2010;30:9477–87.
93. Heuvel MP, van den, Sporns O, Collin G, Scheewe T, Mandl RCW, Cahn W, et al. Abnormal rich club organization and functional brain dynamics in schizophrenia. *JAMA Psychiatry*. 2013;70:783–92.
94. Constantinides C, Han LKM, Alloza C, Antonucci LA, Arango C, Ayasa-Arriola R, et al. Brain ageing in schizophrenia: evidence from 26 international cohorts via the ENIGMA Schizophrenia consortium. *Mol Psychiatry*. 2023;28:1201–9.
95. Aboud KS, Huo Y, Kang H, Ealey A, Resnick SM, Landman BA, et al. Structural covariance across the lifespan: Brain development and aging through the lens of inter-network relationships. *Hum Brain Mapp*. 2018;40:125–36.
96. DuPre E, Spreng RN. Structural covariance networks across the life span, from 6 to 94 years of age. *Netw Neurosci*. 2017;1:302–23.
97. Rakic P. Evolution of the neocortex: a perspective from developmental biology. *Nat Rev Neurosci*. 2009;10:724–35.
98. Zhou J, Seeley WW. Network dysfunction in Alzheimer's disease and frontotemporal dementia: implications for psychiatry. *Biol Psychiatry*. 2014;75:565–73.
99. Feinberg I. Schizophrenia: caused by a fault in programmed synaptic elimination during adolescence? *J Psychiatr Res*. 1982;17:319–34.
100. Stephan KE, Baldeweg T, Friston KJ. Synaptic plasticity and disconnection in schizophrenia. *Biol Psychiatry*. 2006;59:929–39.
101. Frick LR, Williams K, Pittenger C. Microglial dysregulation in psychiatric disease. *Clin Dev Immunol*. 2013;2013:608654.
102. Fillman SG, Cloonan N, Catts VS, Miller LC, Wong J, McCrossin T, et al. Increased inflammatory markers identified in the dorsolateral prefrontal cortex of individuals with schizophrenia. *Mol Psychiatry*. 2013;18:206–14.
103. Do KQ, Cabungcal JH, Frank A, Steullet P, Cuenod M. Redox dysregulation, neurodevelopment, and schizophrenia. *Curr Opin Neurobiol*. 2009;19:220–30.
104. Steullet P, Cabungcal J-H, Coyle J, Didrikens M, Gill K, Grace AA, et al. Oxidative stress-driven parvalbumin interneuron impairment as a common mechanism in models of schizophrenia. *Mol Psychiatry*. 2017;22:936–43.
105. Nakazawa K, Sapkota K. The origin of NMDA receptor hypofunction in schizophrenia. *Pharmacol Ther*. 2020;205:107426.
106. Pasternak O, Westin C-F, Bouix S, Seidman LJ, Goldstein JM, Woo T-UW, et al. Excessive extracellular volume reveals a neurodegenerative pattern in schizophrenia onset. *J Neurosci*. 2012;32:17365–72.
107. Tang Y, Pasternak O, Kubicki M, Rathi Y, Zhang T, Wang J, et al. Altered cellular white matter but not extracellular free water on diffusion MRI in individuals at clinical high risk for psychosis. *AJP*. 2019;176:820–8.
108. Abbasi S, Wolff A, Çatal Y, Northoff G. Increased noise relates to abnormal excitation-inhibition balance in schizophrenia: a combined empirical and computational study. *Cereb Cortex*. 2023;33:10477–91.
109. Hagmann P, Cammoun L, Gigandet X, Meuli R, Honey CJ, Wedeen VJ, et al. Mapping the structural core of human cerebral cortex. *PLoS Biol*. 2008;6:e159.
110. Bassett DS, Bullmore E. Small-World Brain Networks: The Neuroscientist. 2016. 29 June 2016. <https://doi.org/10.1177/1073858406293182>.
111. Ottet M-C, Schaer M, Debbané M, Cammoun L, Thiran J-P, Eliez S. Graph theory reveals dysconnected hubs in 22q11DS and altered nodal efficiency in patients with hallucinations. *Front Hum Neurosci*. 2013;7:402.
112. Lefort-Besnard J, Bassett DS, Smallwood J, Margulies DS, Derntl B, Gruber O, et al. Different shades of default mode disturbance in schizophrenia: Subnodal covariance estimation in structure and function. *Hum Brain Mapp*. 2018;39:644–61.
113. McGorry PD, Purcell R, Hickie IB, Yung AR, Pantelis C, Jackson HJ. Clinical staging: a heuristic model for psychiatry and youth mental health. *Med J Aust*. 2007;187:540–2.
114. Martínez-Cao C, de la Fuente-Tomás L, García-Fernández A, González-Blanco L, Saiz PA, García-Portilla MP, et al. Is it possible to stage schizophrenia? A systematic review. *Transl Psychiatry*. 2022;12:197.
115. Hickie IB, Scott EM, Hermens DF, Naismith SL, Guastella AJ, Kaur M, et al. Applying clinical staging to young people who present for mental health care. *Early Interv Psychiatry*. 2013;7:31–43.
116. Woods SW, Parker S, Kerr MJ, Walsh BC, Wijtenburg SA, Prunier N, et al. Development of the PSYCHS: positive Symptoms and diagnostic criteria for the CAARMS harmonized with the SIPS. *Early Interv Psychiatry*. 2024;18:255–72.
117. Stauffer E-M, Bethlehem RAI, Warrier V, Murray GK, Romero-Garcia R, Seidlitz J, et al. Grey and white matter microstructure is associated with polygenic risk for schizophrenia. *Mol Psychiatry*. 2021;26:7709–7718.
118. Sebenius I, Seidlitz J, Warrier V, Bethlehem RAI, Alexander-Bloch A, Mallard TT, et al. Robust estimation of cortical similarity networks from brain MRI. *Nat Neurosci*. 2023;26:1461–71.
119. World Medical Association. World Medical Association Declaration of Helsinki: Ethical principles for medical research involving human subjects. *JAMA*. 2013;310:2191–4.

ACKNOWLEDGEMENTS

This study was supported by the Singapore National Medical Research Council (NMRC/OFLCG19May-0035, NMRC/CIRG/1485/2018, NMRC/CSA-SI/0007/2016, NMRC/MOH-00707-01, NMRC/CG/435 M009/2017-NUH/NUHS, CIRG21nov-0007 and HLCA23Feb-0004), Research, Innovation and Enterprise (RIE) 2020 Advanced Manufacturing and Engineering (AME) Programmatic Fund from Agency for Science, Technology and Research (A*STAR), Singapore (No. A20G8b0102), Ministry of Education (MOE-T2EP40120-0007 & T2EP2-0223-0025, MOE-T2EP20220-0001), and Yong Loo Lin School of Medicine Research Core Funding, National University of Singapore, Singapore. Professor Ingrid Agartz acknowledges the Research Council of Norway (grant 223272), South-Eastern Norway Regional Health Authority, The Swedish Research Council, and Karolinska Institutet. Professor Paul Allen has received grant UK G0700995 from the UK Medical Research Council. Professor G. Paul Amminger has received multiple grants from the National Health and Medical Research Council. Professor Ole A Andreassen has received grants 223273 and 283798 from the Research Council of Norway as well as grants from K. G. Jebsen

Stiftelsen and UiO: Life Science. Dr Inmaculada Baeza acknowledges Instituto de Salud Carlos III (INT19/00021) for her support. Dr Inmaculada Baeza, Dr Adriana Fortea and Mr Jose C Pariente would like to thank ISCIII (P111/1349, P115/0444, P1180242), “Una manera de hacer Europa”. Professor Stefan Borgwardt has received grants from the SYNCHIZ project under the ERA-NET Horizon 2020 program. Professor Michael WL Chee has received grant NMRC/TCR/003/2008 from the National Medical Research Council Translational and Clinical Research Flagship Programme. Professor Tiziano Colibazzi has received grants 5T32MH15144 and K23 MH85063 from the National Institute of Mental Health as well as grants from the Brain and Behavior Research Foundation, Sackler Institute, Herbert Irving Scholar Award, and Columbia University Bodini Fellowship. Dr Cheryl M Corcoran is supported by R01MH107558 and R01MH115332 from the National Institutes of Health. Dr Vanessa L Cropley has received investigator grant 1177370 and project grant 1065742 from the National Health and Medical Research Council. Professor Camilo de la Fuente-Sandoval was supported by grants 261895 and 320662 from the Consejo Nacional de Ciencia y Tecnología (CONACyT), grants from CONACyT’s Sistema Nacional de Investigadores (SNI), and grant R21 MH117434 from the National Institutes of Health. Ms Montserrat Dolz has received grants P111/02684 and P115/00509 from the Instituto de Salud Carlos III and a grant from the Alicia Koplowitz Foundation. Professor Paolo Fusar-Poli has received grant UK G0700995 from the UK Medical Research Council. Professor Birte Yding Glenthøj was supported by the Lundbeck Foundation Center for Clinical Intervention and Neuropsychiatric Schizophrenia Research. Dr Louise Birkedal Glenthøj was supported by the TrygFoundation; the Danish Research Council on Independent Research; the Lundbeck Foundation Center for Clinical Intervention and Neuropsychiatric Schizophrenia Research, CINS. Dr Shalaila S Haas is supported by NIH National Institute of Mental Health, grant T32MH122394. Dr Kristen M Haut received support from NIMH grant R01MH105246. Dr Rebecca A Hayes has received grants from the University of Pittsburgh Medical Center. Professor Christine I Hooker was supported by grant R01 MH105246 from the National Institutes of Health. Professor Michael Kaess has received grants from German Federal Ministry of Education and Research, Swiss National Science Foundation, German Research Foundation, Dietmar Hopp Foundation, Baden-Wuerttemberg Foundation, and National Health, Medical and Research Council. Professor Kiyoto Kasai received support from JSPS KAKENHI Grant Number JP21H05171 & JP21H05174, AMED under Grant Number JP23wm0625001, and Moonshot R&D Grant Number JPMJMS2021, Japan. Professor Minah Kim has received grant 2019R1C1C1002457 from the National Research Foundation of Korea and grant 21-BR-03-01 from the KBRI basic research program through Korea Brain Research Institute, funded by the Ministry of Science & ITC. Professor Jochen Kindler has received grants from the Swiss National Science Foundation and Lundbeck Foundation. Dr Mallory J Klauinig has received grants from the National Institute of Mental Health. Dr Shinsuke Koike received support from Japan Agency for Medical Research and Development (AMED) under Grant Number JP18dm0307001, JP18dm0307004, and JP19dm0207069, and JST Moonshot R&D (JPMJMS2021). Dr Tina D Kristensen was supported by a Brain and Behavior Research Foundation 2021 NARSAD Young Investigator Grant (ID 30112). Professor Jun Soo Kwon has received grant 2020M3E5D9079910 from the National Research Foundation of Korea and grant 21-BR-03-01 from the KBRI basic research program through Korea Brain Research Institute, funded by the Ministry of Science & ITC. Dr Irina Lebedeva was supported by grant 20-013-00748 from the Russian Foundation for Basic Research. Professor Rachel L Loewy has received grants K23MH086618 and R01MH081051 from the National Institute of Mental Health. Professor Daniel H Mathalon DHM has received grants from the Brain and Behavior Research Foundation and grant R01 MH076989 from the National Institute of Mental Health. Professor Patrick McGorry has received multiple grants from the National Health and Medical Research Council. Professor Philip McGuire has received grant UK G0700995 from the UK Medical Research Council. Professor Romina Mizrahi has received grants R01MH100043 and R01MH113564 from the National Institute of Mental Health and grants from the Brain and Behavior Research Foundation and Canadian Institutes of Health Research. Professor Barnaby Nelson has received Career Development Fellowship grant 1027532, Senior Research Fellowship grant 1137687, and project grant 1027741 from the National Health and Medical Research Council. Professor Takahiro Nemoto has received grants from Otsuka. Professor Merete Nordentoft is supported by Mental Health Center Copenhagen, Mental Health Services in the Capital Region of Denmark, and University of Copenhagen. Dr Dorte Nordholm has received grants R25-A2701 and R287-2018-1485 from the Lundbeck Foundation and grants from the Mental Health Services Capital Region of Denmark. Professor Christos Pantelis was supported by a National Health and Medical Research Council (NHMRC) L3 Investigator Grant (1196508) and NHMRC Program Grant (ID: 1150083). Dr Francisco Reyes-Madrigal was supported by grants from SNI. Professor Wulf Rössler has received grants from the Zurich Program for Sustainable Development of Mental Health Services. Professor Dean F Salisbury was supported by the National Institutes of Health, R01 MH113533. Dr Daiki Sasabayashi has received grant JP18K15509 and JP22K15745 from the JSPS KAKENHI. Professor Ulrich Schall has received grant 569259 from the National Health and Medical Research Council of Australia. Professor

Gisela Sugranyes is supported by the Fundació Clínic Recerca Biomèdica, the Brain and Behavior Research Foundation (NARSAD Young Investigator Award 2017, grant ID: 26731), the Alicia Koplowitz Foundation and the Spanish Ministry of Health, Instituto de Salud Carlos III “Health Research Fund” (P115/0444; P118/0242; P118/00976; P12100330). Professor Michio Suzuki has received grant JP20H03598 from the Japan Society for the Promotion of Science KAKENHI and grant JP19dk0307069s0203 from the Japan Agency for Medical Research and Development. Dr Tsutomu Takahashi was supported by JSPS KAKENHI Grant Number JP18K07550. Professor Christian K Tamnes is supported by the Research Council of Norway (#223273, #288083, #323951) and the South-Eastern Norway Regional Health Authority (#2019069, #2021070, #2023012, #500189). Professor Jinsong Tang has received grant 81871057 from the National Natural Science Foundation of China. Mr Alexander S Tomyshev was supported by grant 20-013-00748 from the Russian Foundation for Basic Research. Dr Jordina Tor has received grants P111/02684 and P115/00509 from the Instituto de Salud Carlos III. Professor Peter J Uhlhaas has received grant MR/L011689/1 from the UK Medical Research Council. Dr James A Waltz has received grant 5R01MH115031 from the National Institute of Mental Health. Professor Lars T Westlye received European Union’s Horizon 2020 Research and Innovation Program grant 802998 from the European Research Council. Professor Stephen J Wood has received grant 566529 and a Clinical Career Development Award (359223) from the National Health and Medical Research Council. Professor Alison R Yung has received multiple grants from the National Health and Medical Research Council. Professor Paul M Thompson is supported in part by NIH grants R01MH123163, R01MH121246, and R01MH116147. Core funding for ENIGMA was provided by the NIH Big Data to Knowledge (BD2K) program under consortium grant U54 EB020403 to PMT. Dr Maria Jalbrzikowski is supported by NIMH grants K01MH112774 and R01MH129636. Dr Jimmy Lee received grant NMRC/TCR/003/2008 from the National Medical Research Council Translational and Clinical Research Flagship Programme. Further, we would like to acknowledge Tomas Moncada-Habib, MD, Philipp G. Sämann, MD, Rachel M. Radisson, MD, and Ranjini RG Garani, MSc.

AUTHOR CONTRIBUTIONS

SL and JZ had full access to all the data in the study and take responsibility for the integrity of the data and the accuracy of the data analysis. Study concept and design: SL, DH, MJ and JZ. The whole ENIGMA consortium collected the data. Database management: MJ, DH and PMT. Data processing, data interpretation or funding (in alphabetical order): IA, PA, GA, OAA, PB, IB, HB, CFB, SB, SC, XC, KKC, SC, TC, REC, CMC, VLC, LH, CFS, MD, BHE, AF, PF, LG, BG, SSH, HKH, KMH, RAH, YH, KH, WH, DH, CIH, LEH, DH, WH, MK, KK, NK, MJ, MK, JK, MJK, SK, TDK, YK, JK, SML, IL, JL, ILL, PLO, AL, SL, RLL, XM, DHM, PM, CM, RM, MM, PM, RMD, DMS, BN, TN, MN, DN, MAO, LO, CP, JCP, JMR, PER, FR, FRM, LFR, JIR, WR, DFS, DS, US, JS, AS, LS, MES, GS, MS, TT, CKT, JT, AT, SIT, AST, JT, PJU, TGV, TAMJvA, DV, EV, SV, JAW, CW, LTW, SJW, HY, LY, ARY, MWC, PMT, and JHZ. Statistical analysis: SL and JZ. Drafting of the manuscript: SL and JZ. Critical revision of the manuscript for important intellectual content: DH and MJ. All authors approved the contents of the paper.

COMPETING INTERESTS

Professor Ingrid Agartz has received lecturer honoraria from Lundbeck. Professor Ole A Andreassen has received personal fees from Lundbeck and Sunovion and has served as a consultant for Cortechs.ai. Dr Inmaculada Baeza has received personal fees from Angelini Pharma, Janssen Pharmaceuticals, and Otsuka-Lundbeck. Professor Bjørn H. Ebdrup is part of the Advisory Board of Boehringer Ingelheim, Lundbeck Pharma, and Orion Pharma; and has received lecture fees from Boehringer Ingelheim, Otsuka Pharma Scandinavia AB, and Lundbeck Pharma. Professor Paolo Fusar-Poli received grants from Lundbeck; personal fees from Angelini Pharma and Menarini Group; and nonfinancial support from Boehringer Ingelheim. Professor Birte Yding Glenthøj has been the leader of a Lundbeck Foundation Centre of Excellence for Clinical Intervention and Neuropsychiatric Schizophrenia Research (CINS) (January 2009 – December 2021), which was partially financed by an independent grant from the Lundbeck Foundation based on international review and partially financed by the Mental Health Services in the Capital Region of Denmark, the University of Copenhagen, and other foundations. All grants are the property of the Mental Health Services in the Capital Region of Denmark and administrated by them. Dr Louise Birkedal Glenthøj has received support from the TrygFoundation; the Danish Research Council on Independent Research; the Lundbeck Foundation Center for Clinical Intervention and Neuropsychiatric Schizophrenia Research, CINS. Professor Kiyoto Kasai has received grants from Novartis, Astellas, Merck Sharp and Dohme, Eli Lilly and Company, Dainippon-Sumitomo Corporation, Eisai, Otsuka, Shionogi, Ono, Tanabe-Mitsubishi, and Takeda; personal fees from Otsuka, Fuji-Film, Yoshitomi, Kyowa, Janssen Pharmaceuticals, Astellas, Meiji Seika Pharma, Sumitomo Dainippon Pharma, and Takeda; and serves on the funding committees of Takeda Science

Foundation and Astellas. Dr Shinsuke Koike has received grants from Agency for Medical Research and Development, Japan Society for the Promotion of Science, the Naito Foundation, and Takeda Science Foundation. Professor Daniel H Mathalon has served as a consultant to Boehringer Ingelheim and Neurocrine. Professor Takahiro Nemoto has received personal fees from Astellas, Eisai, Janssen Pharmaceuticals, Meiji Seika Pharma, Sumitomo Dainippon Pharma, and Takeda. Professor Christos Pantelis has received honoraria for talks at educational meetings and has served on an advisory board for Lundbeck, Australia Pty Ltd. Dr Francisco Reyes-Madrugal has received speaker fees from Janssen (Johnson & Johnson). Professor Wulf Rössler is supported by the Zurich Program for Sustainable Development of Mental Health Services (ZInEP). The donor had no further role in the experimental design, collection, analysis, interpretation of data, writing, and submitting this article for publication. Professor Michio Suzuki had received personal fees from Nakagawa Hospital. Professor Peter J Uhlhaas has received grants from Lundbeck and Eli Lilly UK. Professor Paul M Thompson receives partial research support from Biogen, Inc., for research unrelated to this manuscript. Dr Jimmy Lee has received grants from the Singapore Ministry of Health's National Medical Research Council; honoraria from Otsuka Pharmaceuticals, Sumitomo Pharmaceuticals, Lundbeck Singapore and Janssen Pharmaceuticals. Other authors have no conflict of interest to declare that are relevant to the content of this article.

ETHICS APPROVAL AND CONSENT TO PARTICIPATE

All methods were performed in accordance with the relevant guidelines and regulations. All 31 sites obtained local institutional review board approval. The Institutional Review Board (IRB) at the Boston Children's Hospital also approved the ENIGMA-CHR Repository (IRB-P00043549). Written informed consent was obtained from every participant, or from the participant's guardian for minors. All studies were conducted in accordance with the Declaration of Helsinki [119].

ADDITIONAL INFORMATION

Supplementary information The online version contains supplementary material available at <https://doi.org/10.1038/s41380-025-03304-6>.

Correspondence and requests for materials should be addressed to Juan H. Zhou.

Reprints and permission information is available at <http://www.nature.com/reprints>

Publisher's note Springer Nature remains neutral with regard to jurisdictional claims in published maps and institutional affiliations.



Open Access This article is licensed under a Creative Commons Attribution-NonCommercial-NoDerivatives 4.0 International License, which permits any non-commercial use, sharing, distribution and reproduction in any medium or format, as long as you give appropriate credit to the original author(s) and the source, provide a link to the Creative Commons licence, and indicate if you modified the licensed material. You do not have permission under this licence to share adapted material derived from this article or parts of it. The images or other third party material in this article are included in the article's Creative Commons licence, unless indicated otherwise in a credit line to the material. If material is not included in the article's Creative Commons licence and your intended use is not permitted by statutory regulation or exceeds the permitted use, you will need to obtain permission directly from the copyright holder. To view a copy of this licence, visit <http://creativecommons.org/licenses/by-nc-nd/4.0/>.

© The Author(s) 2025

¹Centre for Sleep and Cognition, Yong Loo Lin School of Medicine, National University of Singapore, Singapore, Singapore. ²Centre for Translational Magnetic Resonance Research, Yong Loo Lin School of Medicine, National University of Singapore, Singapore, Singapore. ³Department of Psychiatric Research, Diakonhjemmet Hospital, Oslo, Norway. ⁴Centre for Psychiatry Research, Department of Clinical Neuroscience, Karolinska Institutet & Stockholm Health Care Services, Stockholm County Council, Stockholm, Sweden. ⁵KG Jebsen Center for Neurodevelopmental Disorders, University of Oslo, Oslo, Norway. ⁶Norwegian Centre for Mental Disorders Research, Institute of Clinical Medicine, University of Oslo, Oslo, Norway. ⁷Dept of Neuroimaging, Institute of Psychiatry, Psychology and Neuroscience, King's College London, London, UK. ⁸WILL chair PSY team, Centre LiNCog, INSERM U-1172, Lille, Haute De France, France. ⁹Centre for Youth Mental Health, University of Melbourne, Melbourne, VIC, Australia. ¹⁰Orygen, Melbourne, VIC, Australia. ¹¹Centre for Precision Psychiatry, Institute of Clinical Medicine, University of Oslo, Oslo, Norway. ¹²Department of Psychiatry and Behavioral Sciences, Boston Children's Hospital, Boston, MA, USA. ¹³Centro de Investigación Biomédica en Red de Salud Mental (CIBERSAM), Instituto de Salud Carlos III, Barcelona, Spain. ¹⁴Department of Child and Adolescent Psychiatry and Psychology, 2021SGR01319, Institute of Neuroscience, Hospital Clínic Barcelona, Barcelona, Spain. ¹⁵Department of Medicine, Institute of Neuroscience, University of Barcelona, Barcelona, Spain. ¹⁶Fundació de Recerca Clínic Barcelona-Institut d'Investigacions Biomèdiques August Pi i Sunyer (IDIBAPS), Barcelona, Spain. ¹⁷Department of Psychosis Studies, Institute of Psychiatry, Psychology and Neuroscience, King's College London, London, UK. ¹⁸NIHR Maudsley Biomedical Research Centre, South London and Maudsley NHS Foundation Trust and King's College London, London, UK. ¹⁹Health Services and Population Research, Institute of Psychiatry, Psychology, and Neuroscience, King's College London, London, UK. ²⁰Department of Psychiatry, University of Basel, Basel, Switzerland. ²¹Department of Psychiatry and Psychotherapy, University of Lübeck, Lübeck, Germany. ²²Department of Psychiatry, University of Pittsburgh, Pittsburgh, PA, USA. ²³Department of Psychiatry, National Clinical Research Center for Mental Disorders, National Center for Mental Disorders, The Second Xiangya Hospital of Central South University, Changsha, Hunan, China. ²⁴National Clinical Research Center for Geriatric Disorders, Xiangya Hospital, Central South University, Changsha, China. ²⁵Department of Psychiatry, Psychiatry Neuroimaging Laboratory, Brigham and Women's Hospital, Harvard Medical School, Boston, MA, USA. ²⁶Department of Brain and Cognitive Sciences, Seoul National University College of Natural Sciences, Seoul, Republic of Korea. ²⁷Department of Psychiatry, Columbia University, New York City, NY, USA. ²⁸New York State Psychiatric Institute, New York City, NY, USA. ²⁹Department of Psychiatry, Harvard Medical School, Cambridge, MA, USA. ³⁰Department of Psychiatry, Icahn School of Medicine at Mount Sinai, New York City, NY, USA. ³¹Mental Illness Research, Education, and Clinical Center, James J Peters VA Medical Center, New York City, NY, USA. ³²Department of Psychiatry, Amsterdam University Medical Centre, Amsterdam, The Netherlands. ³³Arkin, Amsterdam, The Netherlands. ³⁴Laboratory of Experimental Psychiatry, Instituto Nacional de Neurología y Neurocirugía, Mexico City, Mexico. ³⁵Child and Adolescent Mental Health Research Group, Institut de Recerca Sant Joan de Déu, Barcelona, Spain. ³⁶Department of Child and Adolescent Mental Health, Child and Adolescent Psychiatry and Psychology Department, Hospital Sant Joan de Déu, Barcelona, Spain. ³⁷Center for Neuropsychiatric Schizophrenia Research, CNSR, and Center for Clinical Intervention and Neuropsychiatric Schizophrenia Research, CINS, Mental Health Center Glostrup, Glostrup, Copenhagen University Hospital – Mental Health Services CPH, Glostrup, Denmark. ³⁸Department of Clinical Medicine, Faculty of Health and Medical Sciences, University of Copenhagen, Copenhagen, Denmark. ³⁹Department of Psychiatry and Psychology, Institute of Neuroscience, Hospital Clínic Barcelona, Barcelona, Spain. ⁴⁰Early Psychosis: Interventions and Clinical-detection (EPIC) Lab, Department of Psychosis Studies, King's College London, London, UK. ⁴¹Department of Brain and Behavioral Sciences, University of Pavia, Pavia, Italy. ⁴²Outreach and Support in South-London (OASIS) service, South London and Maudsley (SLaM) NHS Foundation Trust, London, UK. ⁴³Department of Psychiatry and Psychotherapy, University Hospital, Ludwig-Maximilian-University (LMU), Munich, Germany. ⁴⁴VIRTU Research Group, Mental Health Center Copenhagen, Copenhagen University Hospital, Copenhagen, Denmark. ⁴⁵Department of Psychiatry & Behavioral Sciences, University of Minnesota, Minneapolis, MN, USA. ⁴⁶Department of Psychiatry and Behavioral Sciences, University of California San Francisco, San Francisco, CA, USA. ⁴⁷Mental Health Service, Minneapolis Veterans Affairs Health Care System, Minneapolis, MN, USA. ⁴⁸Department of Psychiatry and Behavioral Sciences, Rush University Medical Center, Chicago, IL, USA. ⁴⁹Department of Psychiatry and Psychotherapy I, LVR-Hospital Cologne, Cologne, Germany. ⁵⁰Department of Psychiatry, Psychotherapy and Psychosomatics, Psychiatric University Hospital Zurich, University of Zurich, Zurich, Switzerland. ⁵¹Faculty of Social Sciences, University of Stavanger, Stavanger, Norway. ⁵²TIPS Centre for Clinical Research in Psychosis, Stavanger University Hospital, Stavanger, Norway. ⁵³Translational Research Center, University Hospital of Psychiatry and Psychotherapy, University of Bern, Bern, Switzerland. ⁵⁴College of Medicine, Catholic Kwandong University, Gangneung, Republic of Korea. ⁵⁵Department of Child and Adolescent Psychiatry, Center of Psychosocial Medicine, University of Heidelberg, Heidelberg, Germany. ⁵⁶University Hospital of Child and Adolescent Psychiatry and Psychotherapy, University of Bern, Bern, Switzerland. ⁵⁷Department of Neuropsychiatry, Graduate School of Medicine, The University of Tokyo, Tokyo, Japan. ⁵⁸The University of Tokyo Institute for Diversity and Adaptation of Human Mind, The University of Tokyo, Tokyo, Japan. ⁵⁹The International Research Center for Neurointelligence at The University of Tokyo Institutes for Advanced Study, The University of Tokyo, Tokyo, Japan. ⁶⁰Sakura Medical Center, Toho University, Chiba, Japan. ⁶¹Department of Neuropsychiatry, Seoul National University Hospital, Seoul, Republic of Korea. ⁶²Department of Psychiatry, Seoul National University College of Medicine, Seoul, Republic of Korea. ⁶³Department of Psychology, University of Maryland, Baltimore County, MD, USA. ⁶⁴Center for Evolutionary Cognitive Sciences, Graduate School of Art and Sciences,

The University of Tokyo, Tokyo, Japan. ⁶⁵Division of Psychiatry, University of Edinburgh, Edinburgh, UK. ⁶⁶Laboratory of Neuroimaging and Multimodal Analysis, Mental Health Research Center, Moscow, Russia. ⁶⁷Faculty of Behavioural and Movement Sciences, Department of Clinical, Neuro and Developmental Psychology, Vrije Universiteit Amsterdam, Amsterdam, The Netherlands. ⁶⁸School of Population and Global Health, The University of Western Australia, Crawley, WA, Australia. ⁶⁹San Francisco Veterans Affairs Health Care System, San Francisco, CA, USA. ⁷⁰Department of Psychiatry, University of Oxford, Oxford, UK. ⁷¹Douglas Research Center, Montreal, QC, Canada. ⁷²Department of Psychiatry, McGill University, Montreal, QC, Canada. ⁷³Tokyo Metropolitan Matsuzawa Hospital, Tokyo, Japan. ⁷⁴Department for Mental Health Research and Development, Division of Mental Health and Addiction, Vestre Viken Hospital Trust, Drammen, Norway. ⁷⁵Emergency Department, Hospital Fray Bernardino Álvarez, Mexico City, Mexico. ⁷⁶Department of Neuropsychiatry, Toho University School of Medicine, Tokyo, Japan. ⁷⁷Copenhagen Research Center for Mental Health, Mental Health Center Copenhagen, University of Copenhagen, Copenhagen, Denmark. ⁷⁸Department of Youth Psychiatry, Mental Health Research Center, Moscow, Russia. ⁷⁹Hunan Key Laboratory of Psychiatry and Mental Health, the Second Xiangya Hospital, Central South University, Changsha, China. ⁸⁰Neuropsychiatry Theme, Department of Psychiatry, The University of Melbourne, Parkville, VIC, Australia. ⁸¹Florey Institute of Neuroscience and Mental Health, Center for Mental Health, Parkville, VIC, Australia. ⁸²Monash Institute of Pharmaceutical Sciences (MIPS), Monash University, Royal Parade, Parkville, VIC, Australia. ⁸³Magnetic Resonance Imaging Core Facility, Institut d'Investigacions Biomèdiques August Pi i Sunyer, Barcelona, Spain. ⁸⁴Department of Clinical Physiology, Nuclear Medicine and PET, Functional Imaging Unit, University of Copenhagen, Glostrup, Denmark. ⁸⁵Priority Centre for Brain and Mental Health Research, The University of Newcastle, Newcastle, NSW, Australia. ⁸⁶Priority Research Centre for Stroke and Brain Injury, The University of Newcastle, Newcastle, NSW, Australia. ⁸⁷Clinic for Child and Adolescent Psychiatry, University Hospital of Heidelberg, Heidelberg, Germany. ⁸⁸Department of Psychiatry and Psychotherapy, Charité Universitätsmedizin Berlin, Berlin, Germany. ⁸⁹Department of Neuropsychiatry, University of Toyama Graduate School of Medicine and Pharmaceutical Sciences, Toyama, Japan. ⁹⁰Research Center for Idling Brain Science, University of Toyama, Toyama, Japan. ⁹¹Priority Research Centre Grow Up Well, The University of Newcastle, Newcastle, NSW, Australia. ⁹²Department of Psychological Science, University of California Irvine, Irvine, CA, USA. ⁹³Department of Child and Adolescent Psychiatry, Psychiatric University Hospital Zurich, University of Zurich, Zurich, Switzerland. ⁹⁴Division of Mental Health and Substance Abuse, Diakonhjemmet Hospital, Oslo, Norway. ⁹⁵PROMENTA Research Center, Department of Psychology, University of Oslo, Oslo, Norway. ⁹⁶Department of Psychiatry, Sir Run Run Shaw Hospital, School of Medicine, Zhejiang University, Hangzhou, China. ⁹⁷Key Laboratory of Medical Neurobiology of Zhejiang Province, School of Medicine, Zhejiang University, Hangzhou, China. ⁹⁸Imaging Genetics Center, Mark and Mary Stevens Neuroimaging and Informatics Institute, Keck School of Medicine, University of Southern California, Los Angeles, CA, USA. ⁹⁹Department of Child and Adolescent Psychiatry, Charité Universitätsmedizin, Berlin, Germany. ¹⁰⁰Institute of Neuroscience and Psychology, University of Glasgow, Glasgow, UK. ¹⁰¹Early Intervention in Psychosis Advisory Unit for South-East Norway, TIPS Sør-Øst, Division of Mental Health and Addiction, Oslo University Hospital, Oslo, Norway. ¹⁰²Department of Psychiatry and Neuropsychology, Mental Health and Neuroscience Research Institute, Faculty of Health Medicine and Life Sciences, Maastricht University, Maastricht, the Netherlands. ¹⁰³Melbourne Neuropsychiatry Centre, Department of Psychiatry, University of Melbourne & Melbourne Health, Carlton South, VIC, Australia. ¹⁰⁴Neuropsychiatry, The Royal Melbourne Hospital, Melbourne, VIC, Australia. ¹⁰⁵Maryland Psychiatric Research Center, University of Maryland School of Medicine, Baltimore, MD, USA. ¹⁰⁶Department of Psychology, University of Oslo, Oslo, Norway. ¹⁰⁷School of Psychology, University of Birmingham, Birmingham, UK. ¹⁰⁸Department of Psychiatry, Hamamatsu University School of Medicine, Hamamatsu City, Japan. ¹⁰⁹Institute for Mental and Physical Health and Clinical Translation (IMPACT), Deakin University, Geelong, VIC, Australia. ¹¹⁰School of Health Sciences, University of Manchester, Manchester, UK. ¹¹¹Department of Psychosis, Institute of Mental Health, Singapore, Singapore. ¹¹²Lee Kong Chian School of Medicine, Nanyang Technological University, Singapore, Singapore. ¹¹³Department of Electrical and Computer Engineering, Integrative Sciences and Engineering Programme (ISEP), NUS Graduate School, National University of Singapore, Singapore. *A list of authors and their affiliations appears at the end of the paper. ✉email: helen.zhou@nus.edu.sg

ENIGMA CLINICAL HIGH RISK FOR PSYCHOSIS WORKING GROUP

Ingrid Agartz^{3,4,5,6}, Paul Allen^{7,8}, G. Paul Amminger^{9,10}, Ole A. Andreassen^{5,11}, Peter Bachman¹², Inmaculada Baeza^{13,14,15,16}, Cali F. Bartholomeusz^{9,10}, Stefan Borgwardt^{20,21}, Sabrina Catalano²², Michael WL Chee^{1,2}, Xiaogang Chen^{23,24}, Kang Ik K. Cho²⁵, Sunah Choi²⁶, Tiziano Colibazzi^{27,28}, Cheryl M. Corcoran^{30,31}, Vanessa L. Cropley^{9,10}, Lieuwe de Haan^{32,33}, Camilo de la Fuente-Sandoval³⁴, Montserrat Dolz^{13,35,36}, Bjørn H. Ebdrup^{37,38}, Adriana Fortea^{13,16,39}, Paolo Fusar-Poli^{40,41,42,43}, Louise Birkedal Glenthøj⁴⁴, Birte Yding Glenthøj^{37,38}, Shalaila S. Haas³⁰, Holly K. Hamilton^{45,46,47}, Kristen M. Haut⁴⁸, Rebecca A. Hayes¹², Ying He²³, Karsten Heekeren^{49,50}, Wenche ten Velden Hegelstad^{51,52}, Dennis Hernaus¹⁰², Christine I. Hooker⁴⁸, Leslie E. Horton²², Daniela Hubl⁵³, Maria Jalbrzikowski^{12,29}, Michael Kaess^{55,56}, Kiyoto Kasai^{57,58,59}, Naoyuki Katagiri⁶⁰, Minah Kim^{61,62}, Jochen Kindler⁵⁶, Mallory J. Klaunig⁶³, Shinsuke Koike^{58,64}, Tina D. Kristensen³⁷, Yoo Bin Kwak²⁶, Jun Soo Kwon^{26,61,62}, Stephen M. Lawrie⁶⁵, Irina Lebedeva⁶⁶, Jimmy Lee^{111,112}, Imke LJ Lemmers-Jansen^{17,67}, Pablo León-Ortiz³⁴, Siwei Liu^{1,2}, Rachel L. Loewy⁴⁶, Xiaoqian Ma²³, Daniel H. Mathalon^{46,69}, Patrick McGorry^{9,10}, Philip McGuire⁷⁰, Chantal Michel⁵⁶, Romina Mizrahi^{71,72}, Masafumi Mizuno⁷³, Paul Møller⁷⁴, Ricardo Mora-Durán⁷⁵, Barnaby Nelson^{9,10}, Takahiro Nemoto⁷⁶, Merete Nordentoft⁷⁷, Dorte Nordholm⁷⁷, Maria A. Omelchenko⁷⁸, Lijun Ouyang^{23,24,79}, Christos Pantelis^{80,81,82}, Jose C. Pariente⁸³, Jayachandra M. Raghava^{37,84}, Paul E. Rasser^{85,86}, Franz Resch⁸⁷, Francisco Reyes-Madrigal³⁴, Luis F. Rivera-Chávez³⁴, Jan I. Røssberg⁶, Wulf Rössler^{50,88}, Dean F. Salisbury²², Daiki Sasabayashi^{89,90}, Ulrich Schall^{89,90}, Andre Schmidt²⁰, Lukasz Smigielski^{50,93}, Mikkel E. Sørensen³⁷, Gisela Sugranyes^{13,14,15,16}, Michio Suzuki^{89,90}, Tsutomu Takahashi^{89,90}, Christian K. Tamnes^{94,95}, Jinsong Tang^{96,97}, Anastasia Theodoridou⁵⁰, Sophia I. Thomopoulos⁹⁸, Paul M. Thompson⁹⁸, Alexander S. Tomyshev⁶⁶, Jordina Tor^{35,36}, Peter J. Uhlhaas^{99,100}, Tor G. Værnes^{6,101} and Therese AMJ van Amelsvoort¹⁰², Dennis Velakoulis^{103,104}, Esther Via^{35,36}, Sophia Vinogradov⁴⁵, James A. Waltz¹⁰⁵, Christina Wenneberg⁷⁷, Lars T. Westlye^{5,6,106}, Stephen J. Wood^{9,10,107}, Hidenori Yamasue¹⁰⁸, Liu Yuan^{23,24,79}, Alison R. Yung^{109,110} and Juan H. Zhou^{1,2,113}✉